Contents

September 2023

News and Reports

Regulars

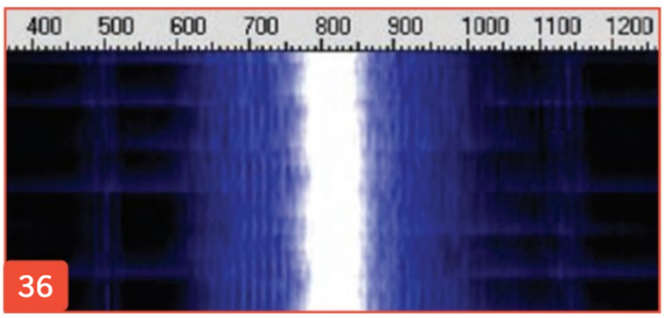

36


72

Features

Technical Features

Reviews

Icom IC-905 review
Design by Kevin Williams, M6CYB

RadCom THE RADIO SOCIETY OF GREAT BRITAIN'S MEMBERS' MAGAZINE
Managing Editor: Edward O'Neill, M0TZX, edward.oneill@rsgb.org.uk
Interim Technical Editor: Peter Duffett-Smith, GM3XJE
Layout and Design: Kevin Williams, M6CYB, kevin.williams@rsgb.org.uk

All contributions and correspondence concerning *RadCom* should be emailed to: radcom@rsgb.org.uk. Alternatively by post to *RadCom* Editor, 3 Abbey Court, Fraser Road, Priory Business Park, Bedford MK44 3WH Phone 01234 832 700.

RadCom is published by the Radio Society of Great Britain as its official journal and is sent free and post paid to all Members of the Society. **The October 2023 edition of *RadCom* is expected to arrive with most Members by 15 September 2023** although this can take up to a week longer in some cases; international deliveries can take longer still.

The online *RadCom* is at www.rsgb.org/radcom/
RadCom Plus is available to RSGB Members online at www.rsgb.org/radcom-plus
RadCom Basics for Members new to the hobby can be found at www.rsgb.org/radcom-basics/
Abbreviations and acronyms we use are listed at http://tinyurl.com/RC-acronyms

RADCOM (ISSN No: 1367-1499) is published monthly by the Radio Society of Great Britain and is distributed in the USA by RRD/Spatial, 1250 Valley Brook Ave, Lyndhurst NJ 07071. Periodicals postage pending paid at So Hackensack NJ. POSTMASTER: end address changes to RADCOM c/o RRD, 1250 Valley Brook Ave, Lyndhurst NJ 07071

www.facebook.com/theRSGB
Twitter @theRSGB

Amateur radio licence revalidation

The RSGB is reminding all radio amateurs that they are required to 'revalidate' their licence at least every five years. In practice, confirming annually is recommended. The process requires every licence holder to confirm or update the details on the Ofcom licence database.

It is important to be registered with, and be able to access, the Ofcom Online Licensing System. This enables revalidation, amendments and other functions including Exam-pass and Special Event callsign applications.

If you are not registered, once you become invalid and exceed a cooling-off period, your callsign becomes potentially available for reassignment to others. Don't let that happen! Keep your details up to date and make a diary reminder to renew each year.

Full Licence note: any 5MHz/60m usage has an explicit licence requirement for a current (preferably mobile) phone number to be stored on the database as well.

Please bear in mind that Ofcom has recently migrated its portal login to a different URL (in case you happened to bookmark it) – not just amateur but also maritime and some other licence types. The new location is: ofcomlive.my.site.com/licensingcomlogin

QSL Matters

Dragons Den

This month's somewhat arresting QSL card caught our eye for a number of reasons, when it landed in the Bureau sort pile recently. A DXpedition card from the Island of Komodo, Indonesia featuring a fearsome lizard, the infamous Komodo dragon, isn't something we come across every day. IOTA island OC-151 has a population of around two thousand people. It is located in the Lesser Sunda chain of the regions 17,507 islands and is home to some 4,000 dragons in the island's national park.

A QRZ.com callsign search revealed that DL3KZA and DL7UVO are no strangers to these islands and neither is Amir, YB9IPY – take a look!

More intriguing is that, although the QSL card is for a DXpedition in 2014, it only arrived with us a few weeks ago. We simply don't know if it has been requested or delayed, but what it demonstrates is that it is always worth ensuring that members have one or two collection envelopes with their QSL volunteer sub-manager at all times.

It is definitely the sort of card to amaze non-amateurs with.

'Receiving cards from the Bureau'

This page on the RSGB website (rsgb.org/main/operating/qsl-bureau/receiving-cards-from-the-bureau/) gives full information and rules for receiving cards from the bureau. It is also repeated in the current *RSGB Yearbook*. If you have never read it, or it has been some time since you last checked, please take a moment to refresh your memory. Doing so would help our volunteers to save much valuable processing time.

A frequent member query is "Why must I use a C5 envelope?" C5 is the largest size that Royal Mail will accept with a standard second-class stamp. Larger envelopes, such as that used for A4 paper, must use the higher value/cost stamp. C5 allows us to send cards of different sizes. The bureau has operated a send-all-send-any policy for each despatch round since 2012, meaning there is little point in affixing a large value stamp to an envelope.

Sub managers have hundreds, or in some cases thousands, of members' envelopes in their filing systems.

Just like any card index, dealing with a single envelope size makes finding the appropriate callsign and Membership number, written on the top left corner, much easier. It is all down to our maxim 'please help us to help you'.

Stamps, the final word

David, G7URP has sent us a timely reminder to advise Members not to attach any more non-bar-coded first- or second-class stamps featuring Her late Majesty Queen Elizabeth II's image to any mail. Doing so would mean that the bureau won't receive the cards as it is unable to pay surcharges.

Through a unique and very special late arrangement, the RSGB negotiated and obtained bar-coded replacement stamps for existing collection envelopes earlier this year, a major logistics exercise.

With one exception, we can no longer accept collection envelopes with non-bar-coded stamps.

David makes the point that stamps featuring other images can still be used for the time being. We recommend that such stamps only be used for sending cards to us and not on collection envelopes that may be with us for some time.

Richard. J. Constantine, G3UGF
QSL Matters

District Representatives for Region 3

The RSGB is looking for members in Region 3, the North-West of England, to step forward as volunteer District Representatives.

If you'd like to make a difference to other radio amateurs in this area, provide advice and support, represent the RSGB and its Members, and also attend local rallies, please email Region 3 Regional Representative, Martyn Bell, M0TEB at: rr3@rsgb.org.uk

GB2RS in Morse!

GB2RS newsreader Graham, G4JBD has developed an online tool which plays Morse code based on the current GB2RS News script at a variety of different speeds. To help simulate a realistic HF-operating environment, the system can be set to include man-made band noise, or QRM, and/or natural band noise, or QRN. To try the system for yourself, visit: thersgb.org/go/gb2rsmorse

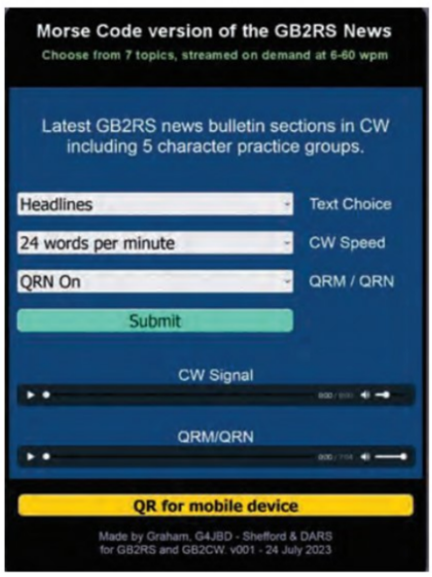

New Products

RF Kit B26-PA HF linear amplifier

Fresh from Friedrichshafen show comes a new 1.5kW HF linear amplifier with internal auto tuner.

- Dual LDMOS devices rated at 3400W ensure a safe operating margin, even at full power.
- Lightweight at only 16Kg
- large 7" (17.8cm) colour display
- <1ms for very fast QSK CW
- In stock and on show at the London showroom.
- £5799.00 Including VAT.

For more information visit the ML&S website: HamRadio.co.uk/RFKit

VX1000-VU tri-band colinear antenna

M0CVO Antennas has a new product – the VX1000-VU tri-band colinear

- Covers 6m, 2m and 70cm.
- With a length of just 1.4m this won't look out of place on any property.

Available from m0cvoantennas.co.uk for £60.95.

JNC Radio SV6301A 1MHz-6.3GHz VNA

Vector Network Analyser covering 1MHz-6.3GHz.

- One of the largest for screen size: 7" (17.8cm) IPS LCD capacitive.
- This really is a beautifully-built instrument supplied in a nice carry case.
- A full video presentation is available on the MLandS.tv YouTube channel.

Available from hamradio.co.uk for £789.95
For more information visit the ML&S website: HamRadio.co.uk/SV6301A

Spiderbeam arrives at Moonraker

Spiderbeam is a German company specializing in the design and manufacture of telescopic fiberglass masts for amateur radio antennas and telecommunication applications.

Founded in 2000 by a group of radio enthusiasts, Spiderbeam is today one of the leading manufacturers of fiberglass masts for amateur radio antennas.

Its telescopic masts are designed to offer high strength and stability, while being light and easy to transport.

They are used by radio amateurs around the world for applications such as shortwave communication, weather monitoring and disaster relief communication.

Spiderbeam products are also used in commercial applications, including environmental monitoring and wireless data communication.

For more information visit moonrakeronline.com

Antennas

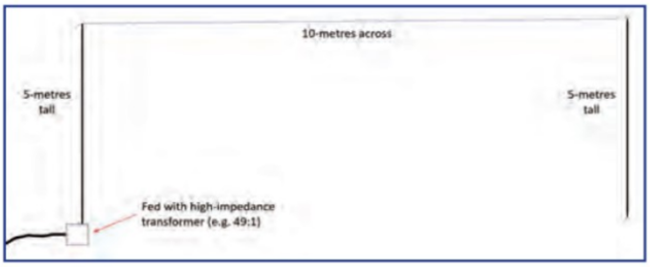

FIGURE 1: **The 'traditional' Half-Square antenna configuration, fed here with a high-impedance transformer at the base of either leg. This example provides us with four harmonically-related bands of operation: 40m, 20m, 15m and 10m.**

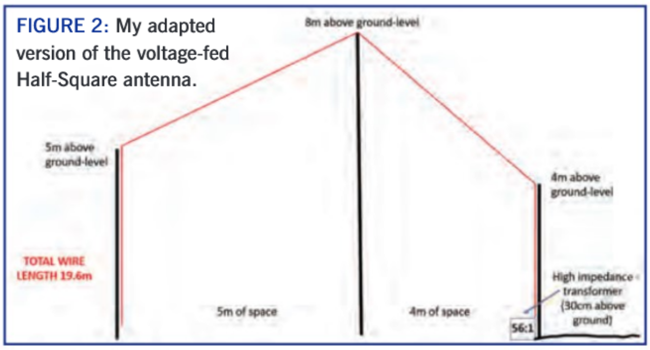

FIGURE 2: **My adapted version of the voltage-fed Half-Square antenna.**

In the past two months we have looked at the Half-Square antenna and how this could be adapted to become a voltage-fed multi-band antenna and how, in theory, the configuration of this antenna could be altered in terms of its height/width ratio and whether the antenna could be configured to cover even more bands.

In this month's article, I will demonstrate how I have adapted this antenna to the special limitations of my QTH, and how the performance of my adapted Half-Square antenna compares with the more traditional configuration.

As a brief reminder, the configuration of the voltage-fed end-fed Half-Square antenna is shown in **Figure 1.** The Half-Square antenna is a full-wavelength of wire, with the traditional configuration being two vertical quarter-wavelength legs at either end, with a half-wave long horizontal wire between them. By feeding with a high impedance transformer at one of its ends, a good match is usually produced for the half-wavelength and its subsequent harmonics. On the full-wavelength frequency (in this case, 14MHz), as these two vertical radiators are being fed in phase with each other, the antenna provides good vertical polarisation, directed broad side to the antenna, useful for DX. On its half-wavelength (7MHz), the Half-Square antenna exhibits useful gain, broad side on, at higher take-off angles, particularly useful for Inter-G and European contacts. On 21MHz, again at low take-off angles, the antenna produces vertical polarisation which mostly surpasses that of a ground-mounted quarter-wave monopole. Finally, on 28MHz, at 5° take-off angle, the Half-Square antenna has good lobes in various directions around the antenna. Peaks in gain are in the corners opposite the feed point (-2.0dBi). Rarely at any point in its azimuth pattern is the gain lower than the -5.9dBi of the omni-directional ground-mounted quarter-wave vertical antenna.

My installation

As we all know, we do not all have the real-estate to erect our first-choice antenna (let alone the antenna farm of our dreams). My QTH has the largest horizontal space of 9m and is without natural supports such as trees. Therefore, my only recourse is to use fibreglass poles. I have chosen to use epoxy glue to secure the telescoping sections permanently together. Because I have the added need, through neighbour considerations on one side of my property, to maintain a visually low-profile antenna system, I have opted to use two side-supporting poles of 4m and 5m in length, each of which are attached to respective boundary fences. To compensate for the short length of horizontal space, I am required to change the traditional flat-top nature of the horizontal section of the Half-Square antenna to an inverted-V shape to save on space. **Figure 2** shows my adapted Half-Square antenna configuration.

FIGURE 3: **The apex of the inverted-V aspect of the antenna, at 8m above ground level.**

The antenna is once again fed with a high-impedance transformer (in this case providing a 56:1 impedance transformation ratio), and is positioned 30cm above the ground near the base of the shorter (4m) of the two supporting fibreglass poles (see **Figure 3**). There are a couple of options as to how to feed this antenna via the transformer. Both options suggest the need to use one or both of a common-mode choke/line isolator somewhere in the coaxial feed line and/or a counterpoise attached to the ground lug of the transformer. My option is to use a line isolator, positioned 7m from the transformer, which chokes back common-mode currents and prevents these from reaching their way into the shack. The 7m length proves effective in terms of allowing a sufficient length of coaxial cable to act as a counterpoise before the choke prevents common-mode currents entering the operating position. A counterpoise could also be used, although I have found that, when using 100W or less on SSB, I have never had any issues when only using a choke on the feed line.

The total antenna length (in my case) is 19.6m. As **Figure 3** shows, my configuration allows for a reasonable peak height of 8m at the apex of the inverted-V, with the far end of the antenna, opposite to the feed-point, terminating at 30cm above ground level (**Figure 4**).

Comparing with the traditional configuration

To assist our comparison between my amended version and the conventional Half-Square antenna, we will be using antenna modelling software (MMANA-gal), along with the usual caveat that each installation has its own unique challenges and influences. Nevertheless, a useful base line can be determined.

On the 40m band, my amended version behaves almost identically to the conventional Half-Square antenna. The azimuth pattern indicates that, when compared with the conventional Half-Square antenna, gain at the inter-G/inter-European useful take-off angle of 70° is only 1dB down on the Half-Square antenna and is omni-directional in nature (see **Figure 5**). As with the conventional design, my amended version has a mixture of horizontal polarisation broad side to the antenna, and vertical polarisation from the

FIGURE 4: The wire opposite the fed-end with it terminated 30cm above ground level.

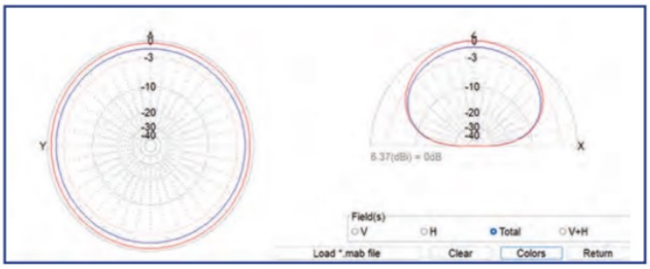

FIGURE 5: On 40m, my adapted version (blue curve) shows just a 1dB reduction in gain at a 70° take-off angle compared with the conventional Half-Square antenna (red curve).

two vertical antenna supports, which accounts for this omni-directionality. Indeed, at the DX-friendly lower angles of 5° take-off angle, a respectable -8dBi gain (vertically polarised) is modelled from both support ends.

On the 20m band, modelled performance is again like the conventional version. As **Figure 6** shows, my amended version has slightly lower gain at 5° in the peak direction broad side on (-3.1dBi compared with -2.7dBi). However, what is noticeable is that the amended design has a more omni-directional pattern, and a higher minimum gain off both far ends (-10.4dBi compared with -13.2dBi).

On the 15m band, there are once again subtle differences between the two designs. As **Figure 7** shows, there are two main lobes at 45° either side from the end opposite the fed-end of the antenna (-2.5dBi). This is slightly greater than the same lobe of the conventional flat-top design. Alternatively, the conventional Half-Square antenna has a slightly-higher gain, again running at 45° and 135° azimuth from the opposite side of the antenna (the fed end).

Figure 8 shows what happens on 10m. It reveals that this is the band where the greatest change occurs between these two antenna designs. The amended version has greater gain than the conventional Half-Square antenna at 45° and 235° azimuth (an increase of 2.5dB). Peak gain is once again at the end opposite the feed point and is vertical in polarisation, measuring -0.8dBi (around 5dB better than a ground-mounted quarter-wave antenna). Broad side to the antenna, the conventional Half-Square antenna now has the slight edge.

Overall, the real-world performance, across all four bands of my amended version of the Half-Square antenna, should not be markedly different from that of the conventional configuration.

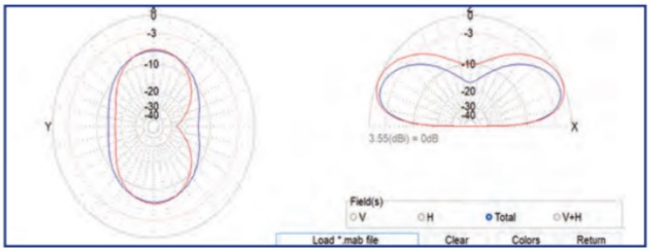

FIGURE 6: On 20m, at 5take-off angle, my adapted version (blue curve) matches the conventional version broad-side on (red curve) and is slightly more omni-directional in nature.

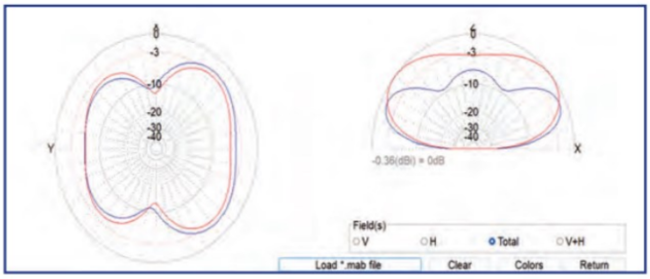

FIGURE 7: On 15m, at 5° take-off angle, my adapted version (blue curve) has slightly greater gain at 45° either side of the far-end of the antenna, and slightly less than the conventional version (red curve) at the same angles from the end fed towards the base.

Erecting, tuning and on the air

With some spare time on a sunny day, I set about putting the antenna together and erecting it. The centre support pole is the bottom eight sections of an inexpensive telescopic fibreglass pole, with the sections having already been secured in place with epoxy glue. Incidentally, this pole has now survived five winters of use. Both side support poles, again fixed with epoxy resin, were then attached to the boundary fences with the antenna wire running to each pole and held in place to run vertically downwards by cable ties at the top of each pole to act as a guide loop for the wire. Around 10.4m of wire was used for each leg and this was then trimmed to fit the available space. On the feed-point side, 9.4m of wire ran from the apex to the transformer and 10.2m of wire from the apex down to the opposite side, totalling 19.6m of wire. On both sides the wire terminated 30cm above ground level.

The VSWR was checked by using a very short piece of coaxial cable (around 30cm in length) attached to the feed point. It would have been ideal to gauge a reading using a double PL259 to attach the antenna analyser directly to the transformer. However, as I did not have one available, a short piece of Aircell 7 coaxial cable was used. I also attached a 12m piece of wire to the ground lug of the transformer. **Table 1** shows the measured VSWR readings near the feed point following shortening the antenna to attempt to move the minimum

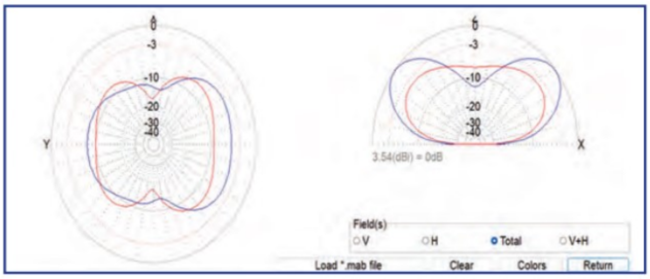

FIGURE 8: On 10m, my adapted version (blue curve) has a peak gain once again at the end opposite the feed point, measuring -0.8dBi. Current here is vertical in direction and is very favourable compared with a quarter-wave or half-wave vertical antenna. Overall coverage in azimuth is competitive compared with the conventional voltage-fed Half-Square antenna (red curve).

Tim Hier, G5TM
timhier@icloud.com

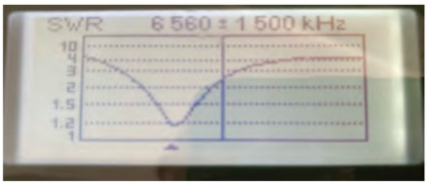

FIGURE 9: The VSWR sweep for 40m.

VSWR on 40m from 6.450MHz up to 7.000MHz. My first instinct was to gradually reduce the length of the antenna and I am glad I only cut 15cm to begin with, as it became noticeable that whilst the VSWR on 20m approached where I desired it to be, on 10m and to a lesser extent 15m, the best VSWR on each band rose to be out of band for 15m and become way above the SSB portion on 10m. Trimming the antenna still further may well bring a good VSWR on 40m and probably 20m but would mean that 15 and 10m would suffer.

Bearing in mind that a higher VSWR creates comparatively greater loss as we rise in frequency, and that a 3.4:1 VSWR produces low loss on 40m with a 12m run of RG-58 coaxial cable, I decided to leave the tuning alone, leaving the VSWR dip at 6.560MHz (**Figure 9**) and relying on the internal tuner of the IC-7300 to match to the feeder. The shack-end VSWR and feed-line losses, based on load VSWR and length/type of feed line, are summarised in **Table 2**. The feed-line loss across all four bands, being under 1dB, was very acceptable and easily accommodated by the rig's internal tuner. The feed line itself consisted of 7m of RG-58 coaxial cable from the transformer to a line isolator, and then a further 5m of RG-58 from the line isolator to the transceiver. The idea here was to use the initial 7m of coaxial cable as a form of counterpoise, and then choke off any potential common-mode currents using the line isolator before the 5m run of coaxial cable to the operating position. I experienced no complications from common mode/RF in the shack using this configuration.

It was typical of course that on the day I was ready to get on the air, that one of the all too recently regular geo-magnetic storms decided to take place. Undaunted, I still made quite a few contacts. Perhaps unsurprisingly, the antenna performed very well on 40m and, with this band opening into the evening, I worked Inter-G and European SSB contacts with great ease using 100W. On 20m SSB, plenty of contacts around Europe were achieved and some DX too, most notably VB2M (Montreal, Canada). There was less activity on 15m, although SSB QSOs were achieved with contacts into Switzerland, Denmark and Spain. The 10m band was largely closed, but two sporadic-E SSB contacts were achieved with Switzerland and Italy, in despite of the rapid and deep QSB remarked upon by all operators concerned.

A key consideration is the noise floor presented to us by this antenna. In my semi-urban QTH, there is a vast potential for neighbourhood devices to wreak havoc with HF reception. On 40m, perhaps remarkably, I find that this antenna is quieter than an inverted-V centre-fed dipole I had previously erected in the same position and had in place for nine months. The noise floor on 40m was S1 to S2 in the daytime, rising to S4 in the evening. On 20m the antenna is noisier (S4), primarily I believe because the antenna on this band has a predominance of vertical polarisation, and that this is noisier at my QTH. On both 15m and 10m, the antenna has a zero S-reading. Please note that for all bands, these measurements were taken without the application of any pre-amplifier. Like all other radio amateurs, I am fully aware that I am only one neighbourly RF-leaky wall-wart or device away from having receive issues to resolve!

Further considerations and observations

There are tweaks and options available to develop this antenna further. Firstly, a compensation coil can be used to help improve the VSWR on 15m and 10m. The coil itself is simply a 1.5μH coil comprising 6 turns of the antenna wire used on a PVC former of around 35mm in diameter. The coil itself should be positioned approximately 1.95m from the transformer. By using this coil, the frequency of minimum VSWR will be lowered on each band by approximately 60kHz on 40m, 170kHz on 20m, 400kHz on 15m, and 1MHz on 10m. It may well be possible, therefore, to provide a better match to 50Ω, especially on the two higher bands, without the need for an ATU, external or within the radio. The antenna itself is likely to be shortened in length by approximately 50cm to 1m following this approach.

It is also possible to add 80m operation using a slightly longer length of wire. By adding a 110μH coil at the far end of the antenna, and a further 2.4m of wire following the coil, a narrow portion (approximately 50kHz) of the 80m band will present a VSWR of 2:1 or better. It is better to add a slightly longer length of wire at the far end of the coil and then trim to bring a good match to the desired portion of the band. Do bear in mind that this wire is short, as a fraction of a wavelength for 80m, so that small adjustments should be made. The internal tuner of any HF transceiver will enable around 100kHz of bandwidth to be used, and a wider-range ATU will provide a still-wider coverage (with accompanying feed line losses). The wire, of course, will need be raised at the far end of the antenna to allow for this extra length and the coil. The coil itself can be constructed using 1mm enamelled copper wire with 260 turns on a 19mm PVC former. This shortened version of the Half-square antenna will be less efficient than a full-sized half-wave dipole for the 80m band, but by how much is less easy to measure. I suggest that 6-12dB would seem plausible. This is not a deal-breaker if it would give you access to 80m and 4 other bands in a space barely one third of a half-wavelength in size. VSWR on 40,20,15 and 10m should remain mostly unaffected.

This antenna, then, is a decent all-round performer, which squeezes into a space that is less than a quarter-wavelength in size for its lowest band, in this case 40m. The greatest overall height used in my instance was 8m above ground, but as we have previously noted, the antenna can be used quite successfully with a minimum height of around 5m, so is suited to a stealthier set up. It is flexible in the sense that it can be adjusted to present a good match to 50Ω using a compensation coil and/or it can be tuned via a transceiver's internal tuner with relatively-low feed-line losses as the transformer reduces the impedance to near 50Ω at the feed point. Its modelled and tested performance is not greatly diminished with some moderate adjustments to its configuration compared with the conventional design. It presents good coverage for short-hop/short-skip on 40m, has achieved DX on 20m, and has distinct potential to do the same on 15 and 10m when these higher bands are open. It can also be extended to give access to the 80m band with less than 3m of further antenna length required.

Almost all multi-band wire antennas suffer under some sort of compromise. The voltage-fed and (in my case) configuration-adjusted Half-Square antenna is no different. But for many amateurs, it ticks lots of boxes for the installation of a small-space low-fuss antenna.

Correspondence

Following my discussion of the Rybakov antenna (June 2023 issue of *RadCom*), I have received an email from a reader who questions whether this antenna would work at all because of its compromised design. Readers of this column might like to refer to www.dxzone.com/dx9907/rybakov-antenna-by-iv3sbe.html and make up their own minds!

Table 1: The measured VSWR near the feed point following a reduction in length.

Band	Frequency (MHz)	VSWR
40m	7.000	3.4:1
	6.560 (best VSWR)	1.2:1
20m	14.175	1.5:1
	14.440 (best VSWR)	1.2:1
15m	21.225	1.9:1
	21.520 (best VSWR)	1.3:1
10m	28.500	2.4:1
	29.740 (best VSWR)	1.6:1

Table 2: Calculated shack-end VSWR and feed-line losses, based on the VSWR at the antenna and the length/type of feed line (I used an online calculator).

Band	Frequency (MHz)	VSWR measured in the shack	Feeder loss (dB)
40m	7.000	3.0:1	0.67
20m	14.175	1.4:1	0.54
15m	21.225	1.7:1	0.73
10m	28.500	1.9:1	0.96

Technical

Coaxial cables part one: how to check them using time-domain reflectometry

FIGURE 1: The square-wave generator and the probe.

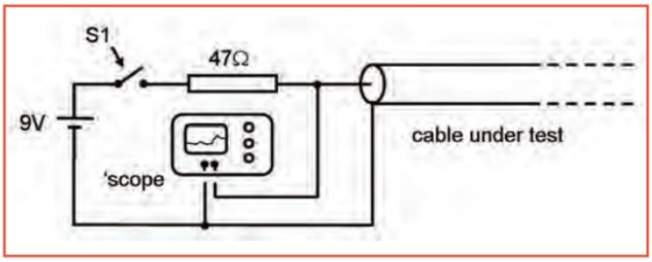

FIGURE 2: A schematic diagram of the circuit I used for testing cables. The switch S1 could be made simply by touching the end of the resistor to the battery.

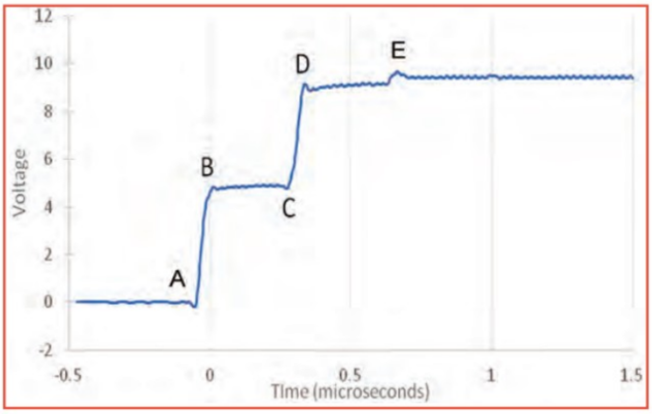

FIGURE 3: Oscilloscope trace from a TDR experiment on my long cable (the cable is terminated with an open circuit).

I hate to have to admit it, but broken wires, short circuits, and similar things are banes of my life, and I expect that they are of yours too.

For example, some time ago I purchased a robot lawnmower. Every year the guide wire breaks somewhere. The best method for finding the break is by using a square-wave generator (1.93kHz) and an audio amplifier with a high input impedance (see **Figure 1**). This can be used to sense the wire even with a small air gap, and I think this kit would be useful for any radio amateur. However, when using it to hunt for faults in coaxial cables there is a problem. The core-to-braid capacitance on the cables give the false impression that the braid is connected to the core, and hence the probe detects the signal everywhere along it. We need to try something else. In particular, I wanted to find a fault (if there was one) in the buried length of RG213 which links my shack to my HF antenna.

One method **[1]** for measuring short leads is to use a capacitance meter, as this can determine if an open circuit is at one end or another. I measured the capacitance of my buried cable to be 3.51nF and, as RG213 has a capacitance of 103pFm^{-1}, this suggested that the cable was about 34m long. The leakage resistance (according to my multimeter) was so high that I could not measure it. Based on these readings, I might have thought that nothing was wrong with the cable, but I wanted to make sure.

I decided to try using time-domain reflectometry (TDR). TDR can be regarded as 'a one-dimensional cable radar'. A pulse is sent down the cable, and is reflected at any point at which the impedance changes **[2]**. The time is measured for the pulse to travel along the cable to the point at which the reflection occurred and then to come back to the start of the cable. Using this time delay, Δt , and the velocity at which signals travel along the cable, the distance to the refection point can be determined.

Using a T-piece, I connected together a pulse generator, the object under test, and my oscilloscope (a PicoScope 2203). You need to choose the pulse generator with care. If the rise time of the pulse is too long, you will not be able to see anything useful with the scope. The rise time needs to be much shorter than the delay time that you are trying to measure. The longer the rise time the greater the uncertainty is in terms of distance long the cable you have. After some experimentation, I found that a good pulse generator was obtained using W2AEW's method **[3]** of using a PP3 battery (9V), a 47Ω resistor, and a switch, in the manner shown diagrammatically in **Figure 2**. You could use a formal switch, as shown in the diagram, or you could simply touch the free end of the resistor to the battery to make the connection.


FIGURE 4: **Measuring 4 x 25m lengths of mains extension leads using TDR.**

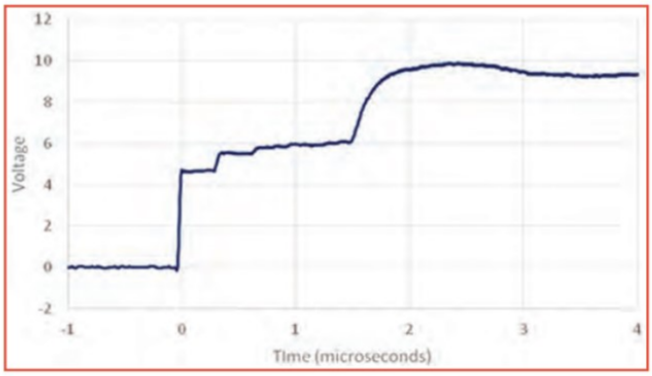

FIGURE 5: **Oscilloscope trace from a TDR experiment on my long cable attached to four 25m mains leads in series.**

Closing the switch sharply applies 9V to the 47Ω resistor. You need to set the 'scope to trigger when the input voltage rises above 1V. This causes it to capture a transient, but you may have to try several times to get a good one.

When I used this with the buried RG213 cable in my garden, I was able to obtain good measurements. These indicated that the cable was in good condition. Here, in **Figure 3**, is an example of such a measurement, and there are several points on the graph of interest, labelled A, B, C, D, and E.

After making the connection to the battery, the voltage starts to increase as shown by the curve between A and B. The rise time is limited mainly by the rise time of the 'scope. At B, the voltage levels off at around 4.5V because, while current flows into the 50Ω coaxial cable, it forms a potential divider with the 47Ω resistor, dividing the 9V roughly by 2. The current continues to flow into the cable between B and C and hence a net flow of energy is going into the cable. The leading edge of the pulse travels down the cable and, at the far end, it is reflected by the open circuit there. At point C, the leading edge of the pulse reaches the near end of the cable again, and adds to the voltage already there, so the voltage rises between C and D. At point D, the cable has already absorbed as much energy as it can, so there is no longer a current flow into the cable and the voltage levels off at the full 9V. Actually, this is not quite true because there is a small mismatch at the near end of the cable (47Ω is not quite 50Ω), so a reflection occurs and a much smaller pulse sets off for the far end again, arriving back at point E.

The time, Δt = 327.5ns between A and C, can be used to measure the length of the cable. We need the speed of light, $c = 3 \times 10^8$ms^{-1}, and the velocity factor of the cable, $\eta = 0.66$, to do this. We can use the following equation to obtain the length of the cable, $x = 32.4$m:

$$x = \frac{c\eta\Delta t}{2}$$

We could, of course, rearrange the equation to measure the velocity factor if we already knew the length.

In TDR, the pulse travels along the cable and, when it reaches a point where the characteristic impedance (Z_0) of the line changes, then part or all of the pulse will be reflected back along the line. The reflection coefficient, Γ, is given by the following equation **[4]**, where Z_L is the impedance of the load (the thing attached to the cable at that point), V_r is the voltage of the reflected wave, and V_f is the voltage of the forwards wave:

$$\Gamma = \frac{Z_L - Z_0}{Z_L + Z_0} = \frac{V_r}{V_f}$$

If Z_L is equal to Z_0, then no reflection occurs ($\Gamma = 0$), and the correctly-terminated line behaves like an infinitely-long line. With Z_L being infinity (open circuit), we get the whole of our voltage wave reflected back at us ($\Gamma = 1$), whilst if it is zero (short circuit), we get the whole of our voltage wave reflected back at us with the voltage wave inverted ($\Gamma = -1$). Things get more complicated when we have lines which are either terminated with moderate mismatches or are lossy.

I continued my experiments (**Figure 4**) by attaching four 25m long PVC-insulated mains extension leads to the end of the long length of RG213 (capacitance of 100m mains lead is 10.9nF). While things like coaxial cables and 300Ω ribbon cable are designed for radio frequencies, things like PVC mains cables are not. The mains cable becomes more lossy as the frequency increases, and the dramatic increase in the losses in the cable with frequency have a strong influence on the shape of the final parts of the transient. **Figure 5** shows the plot on the 'scope in one test.

As before we get a clean step for the RG213 lead. When the signal reaches the first 25m reel of cable, the characteristic impedance change causes a partial reflection. After the first 25m reel, I had connected two reels of a different make of cable in series. You can clearly see a step as the signal passes between the first and the second reel. With the eye of faith, a small step can be seen for the transition to the fourth and final reel. Then a broad, wide step occurs where the signal hits the end of the last reel. This is a much slower rise than the leading pulse at the start of the experiment. It is important to understand that a voltage step is a wide-band event, but the cable response is by no means independent of frequency. You have a mixture of attenuation and dispersion, as well as reflections from changes in impedance. Figure 5 contains a great deal of information, but is difficult to interpret in detail. Note, for example, that the voltage exceeds 9V at about 2.5μs, suggesting the start of a slow transient oscillation.

In my next article, I will write about measurements of cables with a VNA: frequency-domain reflectometry.

References

[1] A. Talbot, Design Notes, *RadCom,* 2013, 99(6), 36-38
[2] H.M. Hashemian and W.C. Bean, Advanced Cable-Testing Techniques for Nuclear Power Plants, *Nuclear Technology,* 2011, 176, pages 414-429, and C. Furse, Y. Chung Chung, C. Lo and P. Pendayala, A Critical Comparison of Reflectometry Methods for Location of Wiring Faults, *Smart Structures and Systems,* 2006, 2(1), 25-46.
[3] Video by W2AEW (#323) https://www.youtube.com/watch?v=z6UJPqQYzNc
[4] H.J. Pain, The Physics of Vibrations and Waves, 3rd Edition, John Wiley and Sons Ltd, Chichester, 1983.

Mark R.StJ. Foreman,
G7LSZ and SA6BID
SA6BID@outlook.com

Rolling HF Blackouts & Solar Flares

An active sunspot region caused numerous HF propagation blackouts in May.

As anticipated in the RSGB's GB2RS propagation report **[1]**, a series of intense solar flares occurred between 18 and 20 May. X-rays from the flares increased the absorption of HF signals in the D-region of the Earth's ionosphere, causing rolling HF blackouts around the world **[2]**.

Figure 1 shows solar x-ray intensity measured by a GEOS satellite on 18-20 May **[3]**. The vertical axis is x-ray flux (W/m^2) vs UTC time. Vertical grey lines indicate 20 M-class flares that caused R1 or R2 level HF blackouts **[4]**. All of the flares were from the same sunspot region (AS3311). **Figure 2** shows estimates of peak HF attenuation in the D-region above London, caused by the three flares highlighted with red arrows in Figure 1. The horizontal axis shows frequency (MHz). The vertical axis shows attenuation (dB) for a single-hop transmission, where an HF signal passes through the D-region once on the way up and again on the way down after refraction. The red line is attenuation by the M8.8 flare at 1235UTC on 20 May (solar zenith angle = 32°); the blue line is for the M5.6 flare at 1500UTC on 20 May (47°); and the green line is for the C6.1 flare at 1240UTC on 19 May (32°). Attenuation is higher at low frequencies. These estimates are from formulas used in the semi-empirical NOAA D-region Absorption Prediction (D-RAP) model **[5]**. The inputs are peak x-ray flux from Figure 1, frequency, and solar zenith angle at the time of the flare. The formulas give attenuation (dB) during a single pass through the D-region.

The D-RAP model is intended as guidance to understand the HF radio degradation and blackouts caused by flares. On the NOAA Space Weather Prediction Center website you can view real-time D-RAP maps and time-lapse animations for the preceding eight hours **[6]**. **Figure 3** shows a global D-RAP map at the peak of the M8.8 flare on 20 May. Color contours show the highest affected frequency (HAF), defined as the highest frequency with 1dB of D-region absorption for two transits. Absorption at lower frequencies is greater than 1dB. In Figure 2 the HAF is the frequency where attenuation is 1dB. The color scale in Figure 3 shows that the HAF in the D-region above London is greater than 30MHz.

The bar chart of attenuation vs frequency at the right side of Figure 3 is for the sol point on the globe, where the sun is directly overhead. This is the point where HF attenuation in the D-region is highest.

Figure 4 shows a global D-RAP map at the peak of the M5.6 flare on 20 May. Compared with the M8.8 flare in Figure 3, the x-ray flux is less intense, and the sun is lower in the London sky (zenith angle = 47°). Nonetheless, the HAF is above 25MHz at London.

Figure 5 shows a global D-RAP map for the C6.1 flare on 19 May at the same time of day as the more intense M8.8 flare on 20 May. The HAF is 18 MHz at London.

The D-RAP documentation notes that absorption estimates can also be scaled up to account for an increase due to oblique incidence at the ionosphere. The correction factor is 1/sin a, where a is the angle of incidence. At vertical incidence a = 9° (Figure 5 in **[7]**).

As solar activity increases, we can expect more rolling blackouts like these.

References

[1] https://gb2rs.podbean.com/

[2] https://www.spaceweather.com Archive: 19 May 2023.

[3] https://www.spaceweatherlive.com/en/solar-activity/solar-flares.html

[4] https://www.swpc.noaa.gov/noaa-scales-explanation

[5] https://www.swpc.noaa.gov/content/global-d-region-absorption-prediction-documentation

[6] https://www.swpc.noaa.gov/products/d-region-absorption-predictions-d-rap

[7] Peter DeNeef, Radio Blackout & Solar Flares, *RadCom*, December 2022, pp 56-57.

Peter DeNeef, AE7PD
HamRadioAndVision@gmail.com

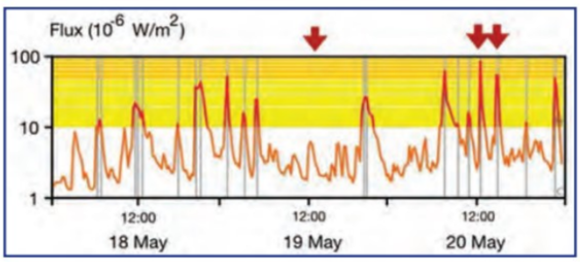

FIGURE 1: X-ray flux from multiple solar flares on 18-20 May. Flux (10^{-6} W/m^2) vs UTC time and date. Vertical grey lines indicate 20 M-class flares. Red arrows indicate the 3 flares analyzed in Figure 2. (Credit: spaceweatherlive.com,reproduced with permission.)

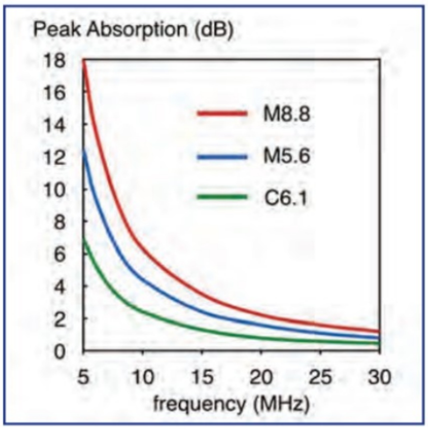

FIGURE 2: Estimates of peak attenuation (dB) in the D-region above London *vs* frequency (MHz) for three solar flares in Figure 1. Red line: M8.8 flare on 20 May. Blue line: M5.6 flare on 20 May. Green line: C6.1 flare on 19 May.

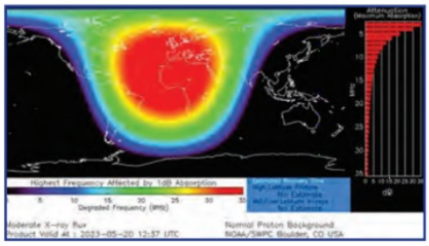

FIGURE 3: Color contours on a NOAA D-RAP global map show the highest frequencies affected by 1dB absorption (HAF) for the M8.8 flare on 20 May [6].

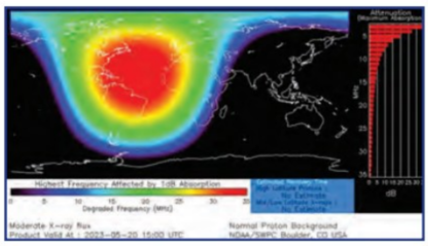

FIGURE 4: D-RAP global map with HAF color contours for the M5.6 flare on 20 May [6].

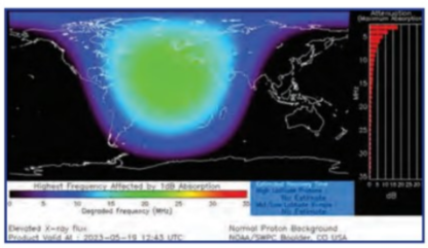

FIGURE 5: D-RAP global map with HAF color contours for the C6.1 flare on 19 May [6].

Insights into HF propagation using FST4W

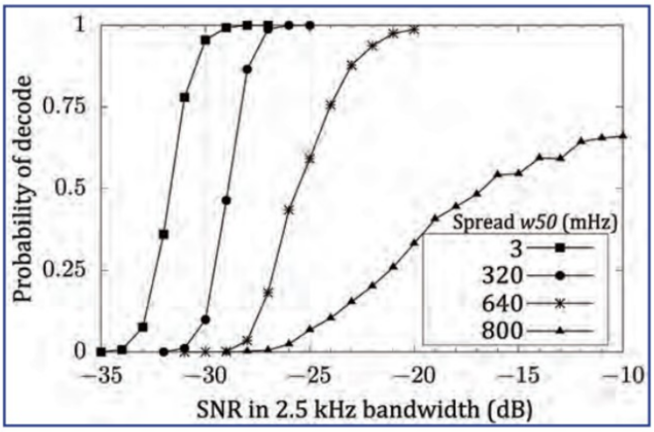

FIGURE 1: Probability of decoding a WSPR signal given SNR and frequency spread, based on an original by Steve Franke, K9AN modified for *w50*.

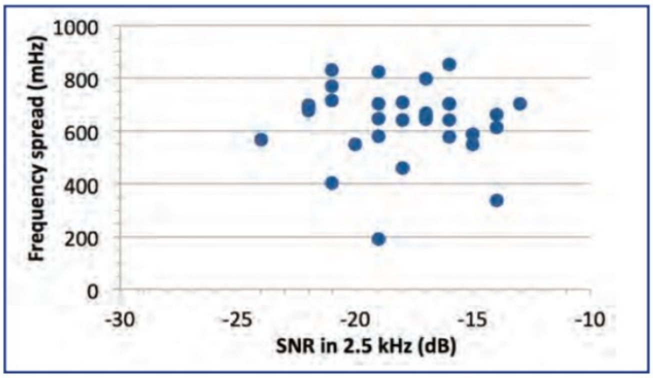

FIGURE 2: Scatterplot of frequency spread against SNR for 14MHz FST4W-120 transmissions from G3ZIL to VY0ERC, Ellesmere Island in February 2023 when Kp high >3. The high spread means that spots with low SNR were not decoded.

I'm a fan of detective fiction and the 'whodunit'. As Sherlock Holmes put it, "Once you eliminate the impossible, whatever remains, no matter how improbable, must be the truth."

Propagation on the HF bands provides me with a rich source of such conundrums. This article takes you through three examples, with information from FST4W, a WSPR-like beacon mode in WSJT-X, providing the clues. Here I concentrate on observations, leaving matching with ray tracing and ionosonde records for later.

WSPR and propagation into the Arctic

This was my first problem. I felt sure it was not lack of signal-to-noise ratio (SNR) preventing my 14MHz WSPR transmissions from Southampton, UK on one day being decoded by VY0ERC at Eureka at 80°N on Ellesmere Island. Ah! The high latitude geomagnetic disturbance index (K high) was five that day. High-speed, about 600km/s, particles originating from a solar storm were steaming down the Earth's magnetic field lines around the north and south geomagnetic poles. Aurora would have been visible. VHF DX operators would have welcomed the event, pointing their beams north to reflect signals from curtains of ionisation in the ionosphere. Unfortunately, these curtains of fluctuating ionisation induce fast flutter and variable Doppler shift into the reflected signals, often termed 'auroral flutter'. Was propagation at 14MHz being affected sufficiently by auroral flutter so as to prevent WSPR signals being decoded? I found a graph of the decode probability with SNR and frequency spread – the variable Doppler shift part of auroral flutter, **Figure 1**.

This was interesting: the oft-quoted SNR threshold for WSPR of less than -30dB in 2.5kHz bandwidth was only possible if the frequency spread was in the order of 3 milliHertz (mHz). This 3mHz frequency spread includes spread arising at the transmitter and receiver as well as spreading by the ionosphere (there are several definitions of frequency spread; here it is *w50*, the width between the half power points). Perhaps *w50* was greater than 800mHz that day? How could I measure *w50*?

Measuring spread with FST4W

The answer was hidden in plain sight. Since release 2.3 in 2021, the well-known WSJT-X package has included a WSPR-like beacon mode, FST4W, that can be configured to measure frequency spread [1 to 4].

The scatterplot of frequency spread against SNR for 14MHz FST4W-120 transmissions (that is, the 120s variant, the same duration and bandwidth as WSPR) from G3ZIL to VY0ERC, **Figure 2**, for K high >3 shows that the SNR had to be at least -24 dB for the high-spread signals to be decoded. It is likely that there were signals received at good SNR that were not decoded because their spread was over 850mHz.

An important implication is that WSPR or FST4W-120, with their small tone spacing of 1.46Hz, may not be useful indicators of propagation for wider-spaced modes such as FT8, or indeed CW, on paths affected by auroral flutter. Wider bandwidth modes are more tolerant of frequency spread.

Number of hops and frequency spread

An experiment with US amateurs showed that combining SNR and frequency spread could identify HF band propagation modes on 14MHz [5]. That is, we could identify the number of hops by the frequency spread. The longer paths proved easier to interpret, and the same approach is taken here. Both examples are on 14MHz and, to assure low spread from the equipment, all master oscillators were GPS disciplined or phase-locked.

Southampton to Fuerteventura – 2700km over sea

The transmitter at Southampton was a QRP Labs QDX digital modes transceiver at 2W modified to use an external 25MHz clock from a phase-locked GPSDO from N6GN [6]. Transmissions were every six minutes. At EA8BFK the receiver was a KiwiSDR with an external 66.66MHz clock from a Bodnar Electronics GPSDO [7] and WsprDaemon software for extended data acquisition [8]. The average sunspot number for 24 to 26 June 2023 was 170. The geomagnetic field was quiet: mid latitude K averaged 3.

The SNR time series, **Figure 3a**, shows that the path was open 24 hours a day. There was significant scatter, with a discernable dip around noon on 25 June. Propagation forecasts predict this dip; it coincided with maximum daily D-layer absorption. Otherwise, there's little information; this is all WSPR (or FT8 etc) would provide.

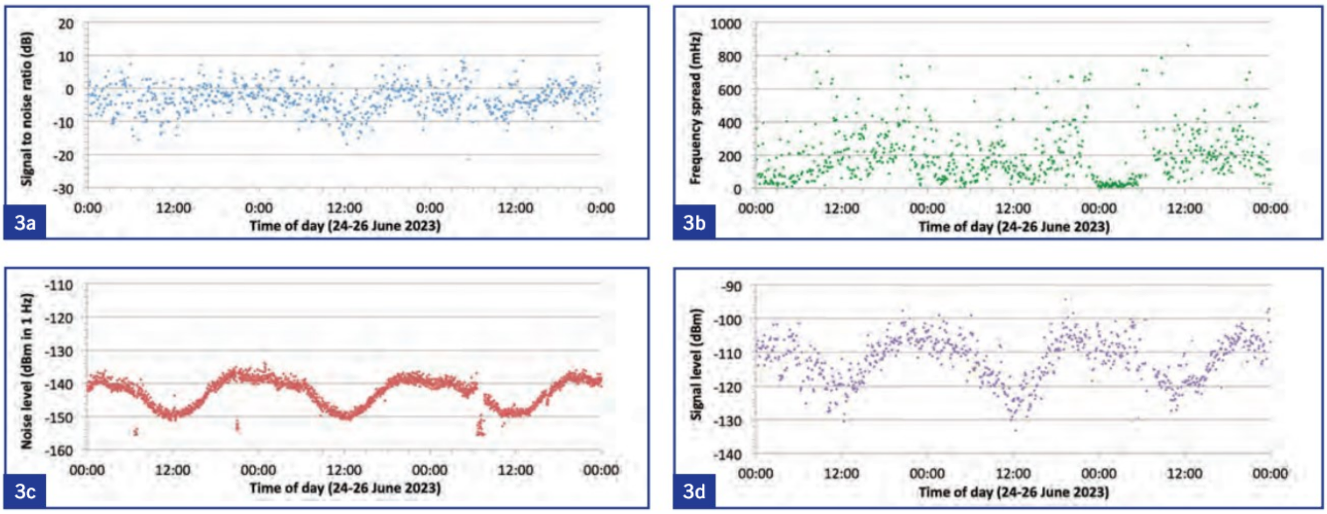

FIGURE 3: Time series of data from a KiwiSDR at EA8BFK, Fuerteventura for 14MHz FST4W-120 transmissions from G3ZIL, Southampton, UK on 24 and 26 June 2023. From top: (3a) SNR in 2.5kHz bandwidth, 3(b) frequency spread *w50* between half-power points, (3c) noise level at the same time and frequency measured using a similar algorithm to that in WSPR, (3d) signal level at the KiwiSDR input calculated from SNR and noise level.

In contrast, the frequency spread time series, **Figure 3b**, is more informative. There are periods of low spread, below 100mHz, and patterns during the periods of higher spread. Low spread occurs during darkness on 24 June and, very noticeably, on 26 June.

While time series are useful in showing when periods with different spread occur, and give times for generating comparative ray traces or comparing with ionosonde records, scatterplots of spread against SNR provide additional insight. **Figure 4** is a scatterplot with non-parametric density contours (as on a map) that help identify peaks in the joint SNR-frequency spread distribution for 26 June. Peak A, with lowest spread, a median of 24mHz, indicated propagation via one-hop between 0000 and 0520UTC.

Peak B, with a median spread of 202mHz, covering most spots, indicated two-hop propagation. It's an effect we saw in the US data **[5]**: two-hop propagation with a land or sea reflection had over twice the frequency spread of one-hop. With less certainty, peak C may have been three-hop propagation.

As an aside, WsprDaemon measures noise in the same band as WSPR / FST4W every two minutes. The noise level at 14MHz at EA8BFK, **Figure 3c**, shows a diurnal variation typical of a site that is limited by propagated-in, rather than local, noise. Around noon, the higher D-layer absorption reduces the propagated-in noise level. Signal level at the receiver input, **Figure 3d**, can be obtained from SNR and noise level. The affect of D-layer absorption on the signal is now much clearer.

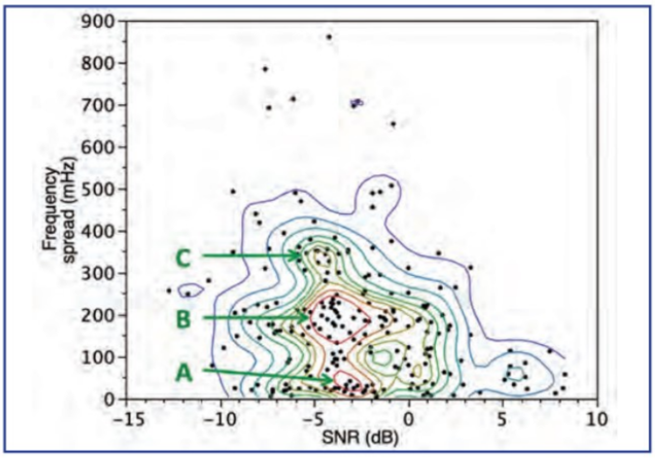

FIGURE 4: Scatterplot of frequency spread against SNR for G3ZIL to EA8BFK for 26 June 2023. Peak A occurred during one-hop propagation, peak B during two-hop and peak C was, possibly, during three-hop propagation. Note that from A to C the SNR at each peak reduced.

Stuttgart to Southampton – 820km

The transmitter at DF4UE, to the east of Stuttgart, was an RFZero with internal GPS-aided clock **[9]** and an external 5W amplifier. G3ZIL used a KiwiSDR receiver, external 66.66MHz Bodnar clock, and WsprDaemon for data acquisition. The morning periods in **Figure 5** with high SNR (median 4dB) and low frequency spread (median 31mHz) were one-hop. But after 14MHz closed for one-hop propagation, there was another mode present. Most clearly present between 1800UTC on 25 June and 0400UTC on 26 June, this mode had low and stable SNR (median -22 dB) and high spread (median 407mHz). It was also present, sporadically, at other times. The scatterplot in **Figure 6** shows just how distinctively different this mode, peak D, was from one-hop, peak A.

The spread for peak D was twice that on the two-hop path UK to Fuerteventura. What was the propagation mode? It is, most likely, two-hop sidescatter, having seen this mode during the US experiment **[5]**. In this under-appreciated mode, the receiver, the blue dot in **Figure 7**, is within the skip zone of the transmitter, the black dot. The small dots are the landing points of rays modelled using the PyLap ray-tracing program in 3D mode **[10]**. Assuming reciprocity holds **[11]**, I place a transmitter at G3ZIL, producing the landing spots in blue. In two-hop sidescatter there is one-hop propagation from the transmitter to the black landing points, sidescatter from ground or sea in the areas of highest overlap, and one-hop propagation to the receiver. For this geometry for DF4UE to G3ZIL the concentrated landing spot overlaps were in southern Spain and, to a lesser extent, northern Scandinavia. Had we been using rotating beams we should have set the headings to those regions, and not for the great circle path.

Gwyn Griffiths, G3ZIL
gxgriffiths@virginmedia.com

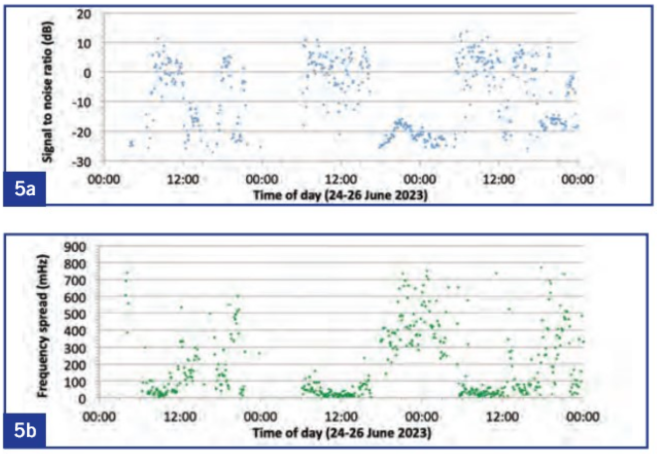

FIGURE 5: Time series of data from a KiwiSDR at G3ZIL for 14MHz FST4W-120 transmissions from DF4UE, east of Stuttgart, Germany on 24 to 26 June 2023. From top: (5a) SNR in 2.5kHz bandwidth, (5b) frequency spread *w50* between half-power points.

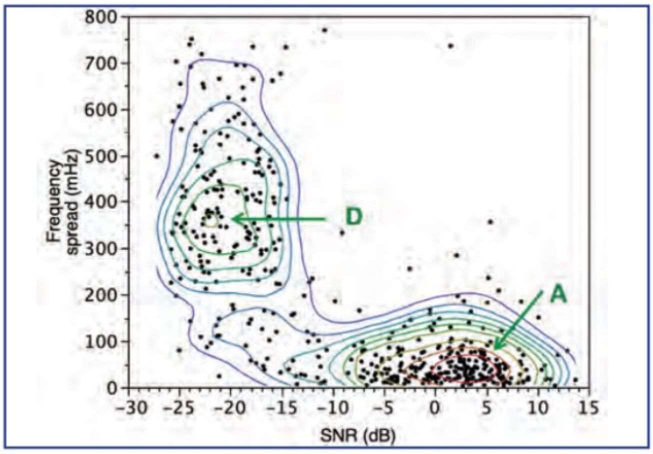

FIGURE 6: Scatterplot of frequency spread against SNR for DF4UE to G3ZIL for 24 to 26 June 2023. Peak A occurred during one-hop propagation, peak D during two-hop sidescatter.

FIGURE 7: Map showing the location of the transmitter at DF4UE (black) and receiver at G3ZIL (blue) together with the landing spots of rays from PyLap 3D ray tracing for 0000UTC on 26 June 2023. It is likely the propagation path was via sidescatter from the regions of greatest landing points overlap.

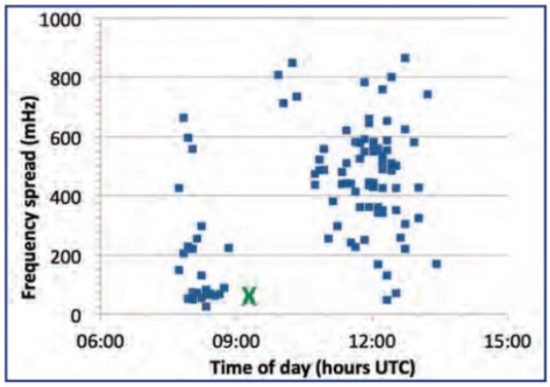

FIGURE 8: Scatterplot of frequency spread against time of day for G3ZIL to K6RFT, Missouri on 14MHz during February 2023. What was the propagation mode for the cluster 'X'?

A conundrum to solve

WSPR is a propagation reporter. I suggest FST4W makes a very useful propagation *analyser*. Turning on its frequency spread measurement capability, and looking at patterns of SNR and spread, fascinating insights into propagation can be gleaned.

I leave you with one of many conundrums. **Figure 8** shows frequency spread against time of day for transmissions on 14MHz from G3ZIL received at K6RFT, Houston, Missouri between 15 and 25 February 2023. Most of the spots around noon could be two, three, or four hop on this 6920km path. But what of the cluster 'X' around 0800UTC, on just one day, 18 February? The median spread was less than 100mHz, and the SNR was higher than for around noon. Over to you...

Acknowledgment

I'm grateful to the WSJT-X development team for FST4W; Rob Robinett, AI6VN for WsprDaemon's extended data acquisition; Pierre Fogal and the Polar Environment Atmospheric Research Laboratory (PEARL) for VY0ERC; Peter Griebel, EA8BFK; Johann Mitrowitsch, DF4UE; Peter Freeman, K6RFT and my US 'Monday morning' friends that have encouraged and contributed to the exploration of FST4W on the HF bands.

References

[1] S. Franke, W. Somerville and J. Taylor. Quick-start guide to FST4 and FST4W, available at https://wsjt.sourceforge.io/FST4_Quick_Start.pdf

[2] G. Griffiths. FST4W on the HF bands: Why - What to expect - Equipment - Results, Proc. ARRL/TAPR Digital Communications Conference 2022, pp. 12–22, available at https://files.tapr.org/meetings/DCC_2022/2022%20DCC1.pdf

[3] R. Tolboom. FST4 Doppler spread algorithm in WSJT-X, available at https://using.tech/posts/fst4/

[4] Members of the WsprDaemon group at: https://groups.io/g/wsprdaemon will be pleased to help new FST4W users.

[5] G. Griffiths. Identifying 14MHz propagation modes using FST4W SNR and spectral spread, accepted by ARRL for QEX.

[6] QDX transceiver at: https://qrp-labs.com/qdx.html and open source hardware from Glenn Elmore at: http://sonic.net/~n6gn/OSHW/

[7] KiwiSDR at http://kiwisdr.com/ (no longer manufactured), Bodnar GPS clock at: http://www.leobodnar.com

[8] The WsprDaemon package from Rob Robinett, AI6VN, decodes WSPR and FST4W spots from KiwiSDRs, audio adapters and the RX888, reports to wsprnet.org and extended data, including FST4W frequency spread to its own database. The code is at: https://github.com/rrobinett/wsprdaemon and full information at http://wsprdaemon.org/

[9] RFZero at: https://rfzero.net/

[10] PyLap is a Python front end to the PHaRLAP ray-tracing program, available at: https://github.com/HamSCI/PyLap

[11] G. Williams, Reciprocity of HF radio waves. *RadCom*, June 2023, p34-35.

Review

RT Systems AT-878 programmer software

Introduction

RT Systems has been in the business of providing third-party programming software for radios since 1995. Manufacturers of radios did not begin providing software to program their radios until about ten years later. Some manufacturers provided software which was more reliable than that provided by other manufacturers and, in some cases, the design was rather idiosyncratic. So, for people who became frustrated trying to do what they wanted to do with each manufacturer's free software, RT Systems software became the 'go-to' for people happy to pay a little to get software that worked more consistently and reliably.

RT Systems cut their teeth on programming software for analogue radios, and I didn't realise until recently that they had moved into the market of providing software for DMR radios. After all, manufacturers of DMR radios really must provide programming software for their radios, because DMR brings an amount of programming complexity not seen in analogue models. If you've listened to DMR for more than a few minutes, you'll probably have heard the word 'codeplug' mentioned. A codeplug, in reality, is nothing more than a configuration file which you load into a radio with all of the set-up information that it needs to make the radio do what you need it to do in terms of channel configurations and so on.

Although DMR radios do come with programming software, as I mentioned above, it can be of varying quality; some software doesn't allow you to copy and paste channel information from one channel to another; other software doesn't make it easy to import and export channels and other information. RT Systems has tried to bring some rigour to the software to make it work predictably, thus facilitating the building of some relatively-complicated codeplugs.

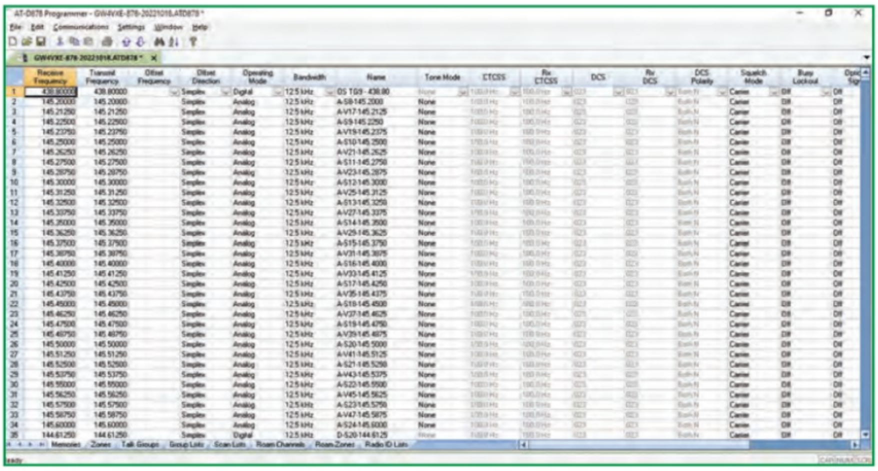

FIGURE 1: The main screen of the programming software.

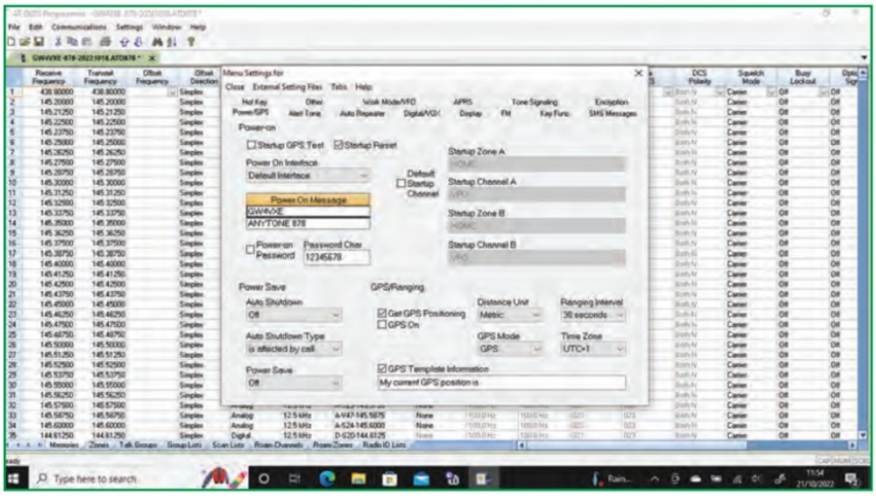

FIGURE 2: The programming software also allows access to configure many options within the DMR Radio.

RT Systems produces programming software for several brands of DMR radios, but they suggested that I have a look at the programmer for the Anytone AT-878 Plus, which happens to be one of my 'go-to' DMR radios. It's a radio which works well, is flexible, and allows me to do what I want to do. Would the RT Systems software work better for me than the software which Anytone produced? Let's see!

RT Systems software

The software is delivered over the internet, as you might expect. Incidentally, the programming software for the Anytone AT-878 is only available for Windows. The software is protected by a serial number which you are sent when you purchase the software.

Installation of the software was very straightforward. I used a Windows 10 machine, but Windows 11 is also supported, along with Windows 8 and 8.1. I wasn't asked to install any separate drivers for the AT-878, so I did wonder if the computer and the radio would talk to each other. Time to find out! I started up the software and pressed 'Read from Radio' to bring the configuration information from the AT-878 onto the computer and into the programming software (see **Figure 1**). This was a good test of communication as well as whether the software was able to read a configuration created by another piece of programming software. Incidentally, I used the programming cable that had come with the AT-878 radio, but RT Systems can also provide a cable which they guarantee will work with their programming software – I had no problems with my Anytone cable.

The configuration information from the AT-878 all came over quickly and loaded into the software without any problems. I saved the file to give me a baseline, in case anything went wrong later on. I find it is a good idea to have a backup, and to check that I can restore from it!

I started to have a look through the different tabs at the bottom of

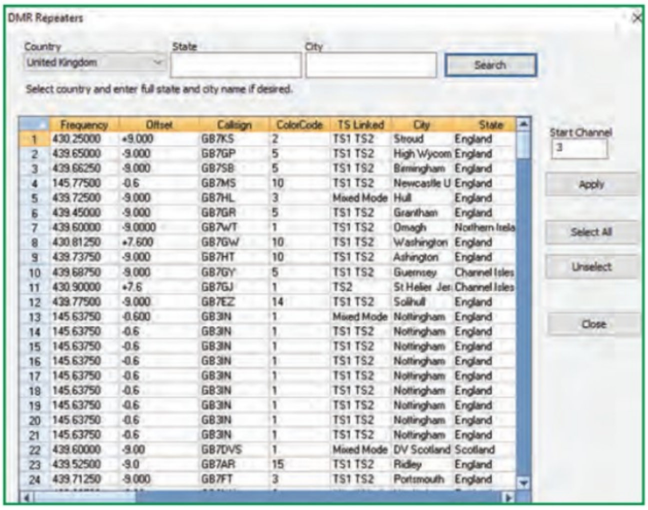

FIGURE 3: The DMR Calculator allows the user to generate a custom codeplug.

the screen, starting with the one containing all the information about memory setup; there are around 1000 memories or channels in my 'comprehensive' codeplug. On experimenting a little, I was pleased to find that I could create a new channel by copying and pasting from another existing channel, and then making whatever changes I needed. Even more pleasing was the fact that I was able to use Control-F (find) on a column to look for particular values (eg the callsign of a repeater). These are small things, but you'd be surprised how much of the DMR programming software fails to implement helpful functionality like this. The programmer also has an analogue mode and a digital mode, accessed under the menu option of 'Edit'. This option hides columns that are not related to the channel information being entered, making it so much easier to sort through. Not only are things not active that are not needed, they are completely hidden.

Something else which the RT Systems software made really easy was downloading contact information into the radio. This is like a directory of callsigns and basic location information mapped against a DMR ID, for example GW4VXE, Tim, Goodwick Pembs, 2353537. If your radio doesn't have this information stored in its contact database, then when you receive my signal, it will just display 2353537, rather than my callsign, name and location. It's nice to be able to refresh your contact database from time to time, but this often involves a couple of bits of software, nothing difficult but it was pleasing that it was readily integrated into the RT Systems software.

I was also really impressed with the software's ability to import repeater information from a variety of sources (*Radio Reference UK, RepeaterBook, RFinder,* web search). You can opt to download all repeater information, say on a particular band for repeaters within 100 miles of your location, and the data will be pulled across. You can then decide which of these repeaters you want to bring into your codeplug and generate a file suitable for import into the AT-878. Or, you can use the 'Repeater List' function, decide which country's data you want to import, and bring it into your list of channels.

Having done this import, you're still going to need to do some work, setting up the appropriate radio ID, talk-groups and so on, but fortunately this is easy to do, making multiple changes at once. There are some very useful editing features within the software (click on 'Help' and select 'Quick Editing Commands'). Column editing is implemented, and this lets you change one item and then paste the change to all channels with only a few mouse clicks. If, for some reason, you need to export data to Excel, this is made simple by the provision of 'Import' and 'Export' functionality.

More features

We've talked about the memories so far, but there are also data tabs for 'Zones' (groups of channels), 'Talk Groups', 'Group Lists', 'Scan Lists', 'Roam Channels', 'Roam Zones' and 'Radio ID Lists', all of which can be maintained through the spreadsheet-like interface.

I wondered whether the various options tabs could also be maintained, as they are in the Anytone software. This includes things like 'Start Up Options', 'APRS', 'Power/GPS', 'Alert Tone', 'Auto Repeater', 'Digital/VOX', 'Display', 'FM', 'Key Function', 'SMS Messages', 'Hot Key', 'Work Mode/VFO', 'Tone Signalling', 'Encryption' and 'Other'. These are indeed included (see **Figure 2**), and I found I had no problem in making changes to these options, uploading them to the radio, and seeing the changes reflected in operation.

The 'DMR Calculator' feature is powerful (see **Figure 3**). Set up the talk groups and zones that you want to use, and then use the 'DMR Calculator' to generate a codeplug automatically, based on repeater input and output frequencies, offsets, colour codes and so on. The calculator allows you to include the talk groups that you want for certain repeaters. This looks particularly useful and will save a lot of manual editing.

Incidentally, although I have described the operation of the software for the Anytone AT-878, a good number of other DMR radios are supported (by different versions of the software); see https://www.rtsystemsinc.com/DMR-Radios_c_914.html for details. Don't forget though, if you have multiple DMR radios, you'll need to purchase a different copy of the programming software for each unit. The good news is that files are interchangeable between the different RT Systems radio programmers, so a file that you create with the Anytone AT-878 programmer could be opened by the RT Systems programmer for the Anytone AT-578 and uploaded to your AT-578 mobile.

Updates to the programming software are issued from time to time, so it is worth clicking on 'Help' and selecting 'Check for Updates' to see if a new version of the software is available.

Final remarks

So, why would you spend $25 on this software when you can use the Anytone software for free? I think you would do so if you wanted to build a relatively-complex codeplug for yourself, rather than downloading a codeplug from a vendor's website, making a couple of changes and uploading it into your radio. The RT Systems software makes it much easier to build the codeplug for yourself, gathering information from the web and importing it.

For those who have a deep interest in DMR programming, you will most likely get some benefit from this software. I have used some DMR programming software which really felt like it was a fight to get things working. The RT Systems software was the opposite of this and did what I wanted and expected. Depending on how much time you spend programming your DMR radio, it could be $25 well spent. The other reason that the RT Systems software could be very useful is that the programming software for some manufacturers seems to have a habit of vanishing from the web. I was recently trying to help a friend with programming a DMR hand-held radio that was popular about three or four years ago; alas, the original software was no longer on the web! RT Systems still had their version available, so it could be a real life-saver in that circumstance, and you wouldn't need to fiddle around with the Prolific USB drivers, which can be a fraught process.

The software can be purchased at https://www.rtsystemsinc.com

Tim Kirby, GW4VXE
gw4vxe@icloud.com

Design Notes

ALC and drive levels

Just about every transceiver incorporates automatic level control (ALC). Its purpose is to control the output power from a transmitter to avoid the power amplifier (PA) stages going into non-linearity or overdrive, typically on SSB speech peaks, but more generally for however the transmitter is driven. It works by sampling the output RF power, P_{OUT}, rectifying this, then feeding a voltage back to control the gain of one of the low-level driver stages. The net result, if it worked exactly as described above, would be a constant power output whatever was put into the audio input socket, with the gain being constantly adjusted to maintain a fixed P_{OUT}. For speech, this is very definitely what we don't want! We need the peaks of the speech waveform to reach the maximum, the peak envelope power (PEP), that the transmitter is designed for, or that we desire, while much of the time the mean output power is much lower.

The achieve this, the rectified sample voltage is applied to a 'hold' circuit. A short speech peak gives a peak in the RF level which is detected and held for a period so that, after feedback, the gain of the driver remains constant for that speech syllable, or several syllables. The delay period is usually a few hundreds of milliseconds so normal speech with pauses can be followed with minimal change in gain. The attack time to respond to a peak needs to be quite short, typically tens or hundreds of microseconds. It has to be rapid, as short overloads of the output stages have considerable potential for causing interference and splatter. The 'output power' control on the front panel of your radio usually adds a back-off voltage to that fed back from the PA, so the gain is never allowed to get high enough to generate more power than demanded, and if it tries to, ALC action takes over to lower P_{OUT}.

The hold delay in the feedback control loop means we have a non-linear system, and any non-linear system causes *some sort* of distortion. For normal SSB, that distortion manifests as a slow flattening of the speech waveform amplitude over many syllables, which is exactly what we want, so in this case the distortion is 'good'. For data waveforms fed in as audio to the microphone socket or an auxiliary socket, ALC is often bad news. Modulation types that have a strong amplitude component, like PSK31, can be damaged if ALC tries to change the amplitude during transmission. PSK31, which has a symbol period of 32ms, is possibly one of the worst affected. For repeated changing symbols, like the idling waveform of binary '1010101010', the amplitude changes smoothly over each symbol in a half-sinusoidal shape. The mean output power is exactly half the peak, or PEP, and is the same for each consecutive symbol. So with an ALC delay covering several symbols, it may work more or less as intended. But as soon as real traffic starts, patterns of consecutive '1's or '0's can appear, and in this case there is no amplitude variation over periods of a significant portion of a second. Now the ALC operates to bring down that part of the waveform, leading to a squashing of the amplitude transitions, in turn leading to degradation of the decoding process and errors appearing. The advice with PSK31 was always to operate with no ALC at all, at a mean power output when idling of no more than one quarter to one half of your transmitter's specified value.

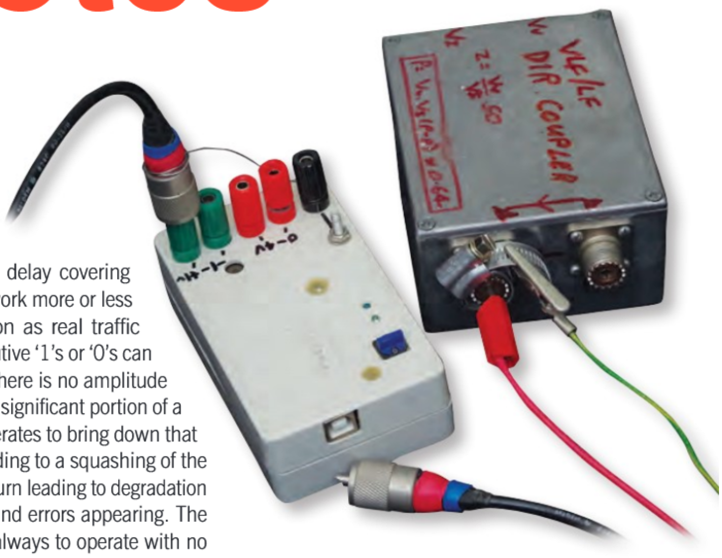

FIGURE 1: The 'shielded banana plug' in use.

Constant-amplitude modes

Different rules apply when the audio drive waveform is constant in amplitude. All the WSJT modes, including the ubiquitous FT8, use multiple frequency shift keying (MFSK) where the transmitted audio, and hence RF, moves from one frequency to the next, always keeping a constant amplitude. So the ALC has nothing to do, you'd think. For slow modes, with one minute or longer cycles like Q65 and WSPR, that's certainly the case, but on FT4 with its 7.5s Tx/Rx cycle times, and to an extent FT8 at 15s, ALC can still poke its nose in. Those two waveforms apply an amplitude ramp at the start and end of transmission to avoid generating transients and causing QRM to adjacent signals. ALC, with its fast attack, can detect this ramp and tries to correct it, reintroducing the rapid transitions the designers attempted to kill. So the advice is try to work with no, or restricted, ALC when using data modes.

The folklore and confusion over ALC can be summed up by this post sent to the WSJT IO-Group: "*I know the ALC has something to do with limiting output power when you turn the RF PWR knob down. As you turn the RF PWR knob down it increases ALC for the given audio input to hold the power output down, so I'm not really clear on whether there is any distortion if there is any ALC action. I've always operated with the WSJT PWR slider pulled down that far acting as the RF power limiter with no ALC action at all, thinking I was doing right. And so far it seems to be working, but if it's true that my audio input to the rig will become distorted from doing that then I need to rethink my setup. I'll reread and apply the audio setup instruction instructions and see what that'll do for me.*"

Mike Black, W9MDB, one of the authors of the WSJT-X software, replied to that post with this generalised set of instructions for setting audio and RF drive level (referring to a nominal 50W transceiver in this case):

#1 Set rig at 50W.
#2 Set WSJT-X 'Pwr' slider at -3dB (this SHOULD show 25W when transmitting, - 3dB is half power).
#3 Set computer playback volume at 0dB.
#4 Press 'Tune' – 25W should be showing.
#5 Adjust rig audio input level so 25W is showing.
#6 Look at the ALC level – probably shows zero at this point when 'Tune' is active.
#7 Start turning up the 'Pwr' slider in WSJT-X – you can click on it and use the cursor up/down keys to change it easily.
#8 Observe when ALC kicks in. It will either be around 45W or not at all by the time you reach 50W.

Mike adds: "I've not seen a rig yet that can't do 90% of the rig's power (45W) without ALC action. ALC does not mean distortion is being caused. It's just the canary-in-the-cave."

The 'shielded banana plug'

Every radio amateur knows the SO239 / PL259 connector family, sometimes referred to as 'UHF connectors'; they're even mentioned in the syllabus for the licence. Amongst many users of the VHF and higher-frequency bands, they are considered mismatched, useless , wouldn't touch them with a barge pole, why do manufacturers insist on still putting them on VHF / UHF radios, etc, so much so that they are popularly referred to as 'shielded

Andy Talbot, G4JNT
andy.g4jnt@gmail.com

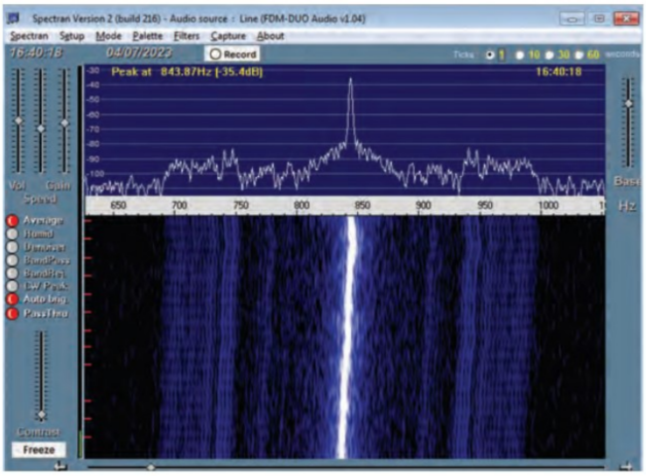

FIGURE 2: Spectrum of the ProgRock2 output multiplied up to 3.4GHz in an ADF4351 synthesizer.

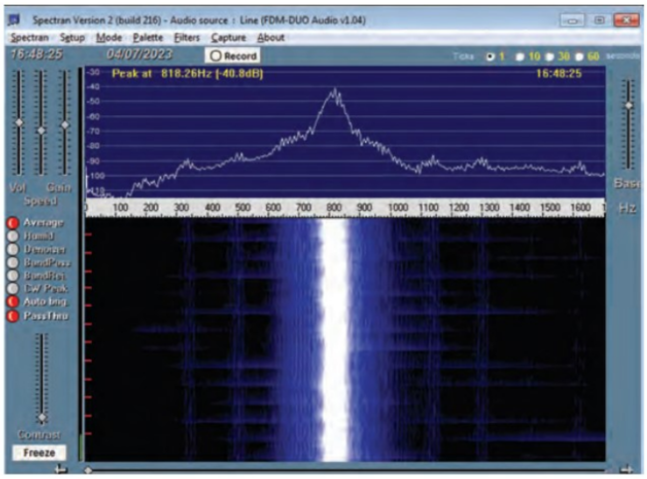

FIGURE 3: The increased spectral width at 3.4GHz with GNSS disciplining applied, after 20-min settling time.

banana plugs' (see **Figure 1**). If this were social media we'd now be showing a smiley face!

But are they really as bad as people claim? For most *practical* purposes, a physical mismatch has to have dimensions of, perhaps, 1/20th of a wavelength or more to be noticed. At 144MHz, that's 10cm. At 432MHz it's 3.5cm. The whole connector isn't that big, so surely it can't be too bad? And mechanically they are quite robust, at least the better-made ones are. They're not waterproof, but self-amalgamating tape solves that. They're usually considered difficult to solder, but there are ways to do the job properly, and compression types that need no soldering abound.

After a discussion on one of the Groups, where all the usual comments were being regurgitated, Dave, G8WBX, who is professionally involved with network-analyser calibration kits and measurement services, made some tests on these 'UHF connectors'. He states "I did a quick bit of checking using these two adapters; * Male PL259 to female N * Male N to female S0239. This was the limit of my testing.

"First I checked the pin depth of the N connectors – mainly so I knew I could mate them with some decent connectors and not cause any damage. Female N was recessed 0.0039in, which is quite reasonable; Male N recessed more than 0.012in, which is the limit of my connector gauges. But the most relaxed N standard allows for recession up to 0.04in if I recall correctly. These connector gauges are for metrology grade connectors, so they don't have the range that general purpose connector gauges would have. So there were no problems there.

"Next I performed the calibration of a HP 8720D VNA from 50MHz to 20GHz. A bit excessive I know, but if someone wanted to play around time-gating, the higher frequency data would be useful.

*Loss for a mated pair of adapters *

- 70MHz 0.001dB
- 144MHz 0.036dB
- 432MHz 0.21dB
- 1.296GHz 0.832dB
- First major suck-out 3.95dB loss at 2.622GHz
- 10.368GHz 3.37dB
- Maximum loss is 7.76dB at 14.9375GHz.

VSWR at female N port 1
- 70MHz 1.05:1
- 144MHz 1.11:1
- 432MHz 1.34:1
- 1.296GHz 1.73:
- 10.368GHz 2.82:1

*VSWR at male N port *2
- 70MHz 1.05:1
- 144MHz 1.11:1
- 432MHz 1.37:1
- 1.296GHz 2.13:
- 10.368GHz 4.63:1"

The tests at 10GHz were more in jest that anything else, but do show the trend. These measurements do seem to bear out the fact that, for practical purposes as far as causing a mismatch, they're almost certainly going to be OK up to 144MHz. But at a measured 1.37:1 VSWR, equating to a rather-poor 16dB return loss on 432MHz, I wouldn't go near one. Of course, if several are cascaded then those mismatches could add and show something even at 144MHz, but probably not worth panicking over. Here at JNT Labs, they're used at LF 137kHz and 475kHz quite deliberately to avoid getting equipment mixed up with the VHF-microwave stuff that uses N-type and SMA connectors. I don't 'do' HF, but if I did they'd probably appear there as well since other HF equipment uses them.

ProgRock2 and the Si5351

A talk at a recent club meeting showed the ProgRock2, a module available from QRP Labs **[1]**. This has a decent temperature-compensated crystal oscillator (TCXO), good for 0.25 parts per million accuracy, driving an MS5351 frequency / timing generator chip which is described as an improved version of the Si5351. The chip can be programmed to provide up to three outputs at arbitrary frequencies, and there is a controller on board that allows frequencies to be set using a USB interface. An added feature of the ProgRock2 is that, by connecting the one pulse per second (1-PPS) signal from a GNSS receiver to an input on the controller, the output frequencies on two of the ports are disciplined, or steered, to GNSS-defined accuracy. This means that they are 'spot-on' when averaged over a long period, but will wander around slightly in the short term because of the disciplining once per second. Only two frequencies are permitted as the third one is forced to be 9.9999995MHz by the frequency-locking process. I was intrigued enough to buy one immediately, not expecting marvellous performance compared with GPS-disciplined oscillators (GPSDO) such as the Leo-Bodnar design **[2]** and several others, but worth a gamble.

To test its short-term stability, the module was programmed to deliver 10MHz on one of its ports (this is the default setting of the unit on delivery) used as a reference for an ADF4351 synthesizer set to deliver 3.4GHz. The ADF4351 has a phase-locked loop (PLL) loop bandwidth of tens of kilohertz, so can be relied upon to faithfully pass all narrow-band artefacts of the ProgRock2 source and multiply these by a factor of 340. A 3.4GHz transverter, using a good quality TCXO as its own local oscillator feeding an

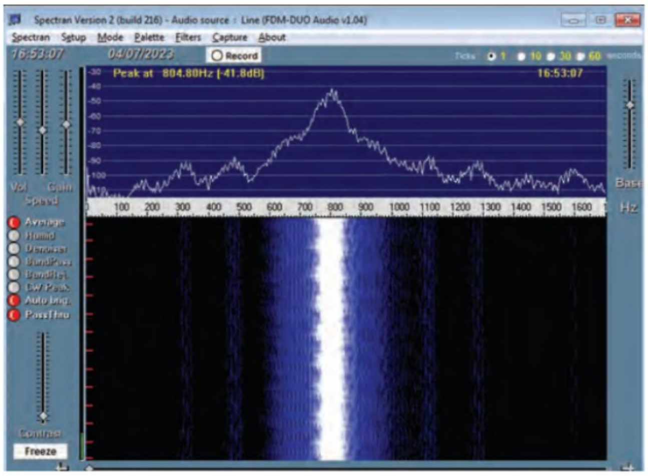

FIGURE 4: GNSS removed, showing how the increased spectral width stays, only reverting to its original state after a reset.

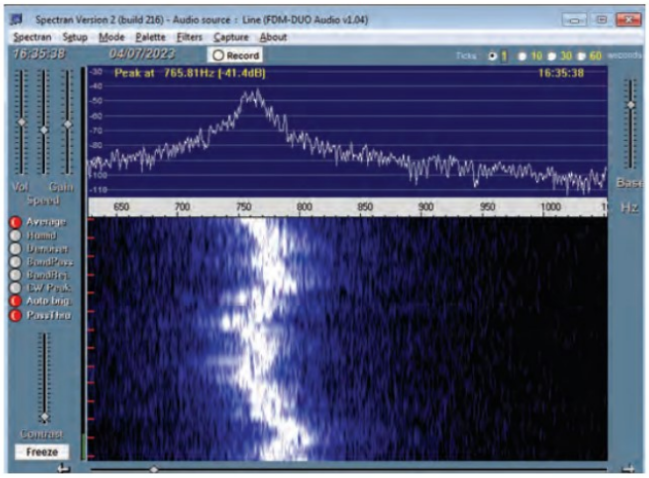

FIGURE 5: Si5351 synthesizer using a free-running 27MHz crystal as its reference, again multiplied to 3.4GHz.

FDM-Duo at 144MHz, was used to monitor the generated signal. The resulting audio was fed into 'Spectran' software to view the spectrum for drift and instabilities.

The first test was made using the ProgRock2 in free-run mode with no GNSS 1-PPS applied. The result is shown in **Figure 2**, where it can be seen the resulting signal is not too bad in terms of stability, with just slight drift. But there is quite a high level of phase noise out to a few hundred hertz around the carrier. This is audible as a slight burble/rumble in the background, but probably wouldn't degrade an SSB contact too badly. It would be fine using typical wide-spaced WSJT-X data modes in use on the microwave bands. The absolute frequency error was around 700Hz at 3.4GHz, 0.2ppm, within specification.

With a 1-PPS signal connected, the audio immediately went wild, hunting in jumps of a few hundred hertz every second as the disciplining process kicked in. After allowing 20min for it to settle down, the jumps reduced considerably and the plot of **Figure 3** is the result. The main lobe of the spectrum shows poor short-term stability with a width of a few tens of Hz, resulting in a louder and more-irritating burble. In addition, audible clicks can be heard every second; these show as the wideband horizontal lines on the plot.

When the 1-PPS signal is removed, the signal does not return to its original almost-clean form, but stays with the same degraded short-term stability, as if it were still being steered by GNSS (**Figure 4**). With artefacts from the 1-PPS signal now gone, phase-noise sidebands from the MS5351 internal PLL synthesizers become apparent. It is clear that, having been steered, the controller is still influencing the TCXO's stability in spite of the 1-PPS having been removed. Switching off then back on restores the cleaner but less stable spectrum of Figure 2.

To compare with an earlier design from QRP-Labs, I borrowed an Si5351 synthesizer module from Paul, M1CNK. This uses a 'real' Si5351 chip but has only a free-running crystal as its reference. The plot from this multiplied to 3.4GHz can be seen in **Figure 5** where it can be seen the short-term stability leaves a lot to be desired if used at that frequency. But it is exactly what would be expected from a standard uncompensated crystal oscillator – a few tenths of a part per million random wobble. And these days, who would ever use a free-running crystal on the microwave bands?

For its original use, as a frequency reference for test equipment, and as local oscillators (LO) and transmitters at LF and HF where QRP-Labs supplies most of its kits, the ProgRock2 is perfectly adequate. That 20Hz spectral width at 3.4GHz is only 80mHz at 14MHz, and no one will notice that in SSB or CW. Even WSPR / FST4 should ride rough shod. But for microwave use, other than for frequency-calibration purposes, the ProgRock2 won't do a good job.

Hunting generators and SMPSUs

Whilst on a walk recently, I stopped off at a mobile coffee and cake waggon at Cheesefoot Head, Winchester, a high spot popular with microwavers. The wagon was being powered from a medium-sized portable generator that looked to be rated around 3kW, possibly more. It appeared quite well made, but I noticed it was hunting badly, with the speed rising and falling all the time in a random manner. On mentioning this to the proprietor, he said "It's an inverter generator, it does that all the time". He didn't seem bothered, it was in regular use for several hours every weekend, so probably OK, but it made me ponder while consuming the good coffee and an excellent flapjack.

Inverter generators usually have an alternator, possibly a car or lorry type for low cost, generating DC via a rectifier, followed by a switch-mode sine-wave inverter to generate 240V AC. These deliver a clean electronically-stabilised output for any arbitrary DC input voltage, within a range that could be quite wide. For any constant-power load, assuming the inverter efficiency remains unchanged, any increase in input voltage will result in a corresponding decrease in input current, the product of V and A remaining constant. The decreasing current with increasing voltage means the converter input exhibits a negative resistance, which can mean stability problems. The alternator itself will have some loss resistance; not a lot, or it would be inefficient. This positive resistance is in series with the negative resistance of the converter, and now things can get interesting. If the sum of the two is a positive value, then the generator will hopefully settle at some speed, probably set by a speed governor, delivering whatever combination of V and A the residual resistance happens to allow at the optimum point on its load line. But, other than a speed governor, there's not much to force whatever combination of V and A it chooses to settle on. If the combined resistance is too low, or is negative, the fun really starts. The spinning mass of the generator is a variable-frequency oscillator damped by the load resistance, with a frequency steered, but not rigidly controlled, by the speed regulator which has a delay in its response. If the damping resistance is too low, we have an unstable situation – a potential oscillator. And this is what's happening. The generator is wandering between any number of values of V and A, the speed control is fighting the rotational mass and not being damped very well by the load resistance, hence the hunting. The 240V output is clean and stable as the converter is doing all the work of stabilising it. Provided the generator mechanics are capable of surviving continual speed changes then no harm is done. It just doesn't sound very healthy.

References
[1] QRP Labs, ProgRock2: https://qrp-labs.com/progrock2.html
[2] Leo Bodnar GPSDO https://www.leobodnar.com/shop/index.php?main_page=index&cPath=107

Icom IC-905

The IC-905 transceiver is the first SHF product from Icom in their 'SHF project'. As well as an overview of the radio's capabilities, we will focus on the features that make it 'stand out from the crowd', particularly the GHz and ATV capabilities.

FIGURE 1: The control unit, and the externally-mounted RF unit (lower), and transverter (upper).

Manufacturer's specifications

Full specifications, including sensitivity and power output on each band band, can be found by reference to Section 11 of the basic user manual, downloadable from [1]. In outline, the manufacturer's specifications are as follows:

- Rx/Tx frequency coverage European version (MHz): 144-146, 430-440, 1240-1300, 2300-2450, 5650-5850, 10000-10500 (with CX-10G transverter)
- Operating modes: USB/LSB (J3E), CW (A1A), RTTY (F1B), AM (A3E), FM (F2D/F3E), DV (F7W), DD (F1D), and ATV (F3F/F8W)
- 500 memory channels (in up to 100 groups)
- Power requirement: 13.8V DC (±15%)
- Operating temperature range: controller 0°C ~ 50°C, 32°F ~ 122°F; RF unit –10°C ~ +55°C, 14°F ~ 131°F
- Frequency stability: better than ±65ppb
- Power consumption on receive standby: 2A (typical)
- Dimensions (not including projections):
  Controller 200 (W) × 83.5 (H) × 82 (D) mm, 7.9 (W) × 3.3 (H) × 3.2 (D) in
  RF unit 172 (W) × 87 (H) × 210 (D) mm, 6.8 (W) × 3.4 (H) × 8.3 (D) in
  Weight of the controller without the supplied accessories: approximately 940g
- Receive system:
  144/430MHz band RF direct sampling
  1200/2400/5600MHz band down-conversion IF sampling
  1200MHz band 1st IF 346MHz band
  2400/5600MHz band 1st IF 914MHz band, 2nd 346MHz band
- Spurious emissions:
  in-band: 144/430MHz below –60dBc, 1200MHz below –53dBc, 2400/5600MHz below –46dBc
  out-of-band: 144/430MHz below –60dBc, 1200MHz below –50dBc, 2400/5600MHz below –43dBc
- Carrier suppression: greater than 50dB
- Unwanted sideband suppression: greater than 50dB

Out of the box

The review transceiver came with all of the interconnecting leads, the 10GHz transverter, and three antennas for 10GHz, 5.7GHz and 2.4GHz. These were simple vertically-polarised collinear arrays housed in radomes, and performance measurements on them are beyond the scope of this review. As horizontal polarisation is the norm on these bands in the UK, it is unlikely that they would be purchased by UK customers at present. Using the equipment with a horizontally-polarised dish antenna, or a panel antenna, is recommended in the UK.

The control unit and the external transverter are shown in **Figure 1**. The control unit has a 'standard' Icom touch-screen user interface so that users of other recent Icom equipment should easily be able to navigate the menus. The external RF unit is noticeably heavy, and has a large heat sink.

No photos have been released of the inside of the transceiver, and we were specifically requested by Icom not to remove the lids to reveal the insides.

Connectors

The transceiver is a multi-unit system, with the main unit covering 144MHz, 432MHz, 1296MHz, 2300MHz and 5760MHz. This consists of an indoor control unit which is connected by a cable to the external RF unit. There is also an additional external transverter for 10GHz. On the outdoor RF unit, there is a female N-type connector for 144MHz, 432MHz and 1296MHz, and separate SMA female connectors for 2.4GHz, and 5.7GHz. There is also an SMA connector for a standard powered GPS antenna, and a BNC female connector for the unit's 10MHz reference output. The separate CX-10 10GHz transverter unit has SMA connectors for its antenna and 2.4GHz IF input, a BNC female connector for its 10MHz reference input, and a pass-through connector to the 2.4GHz antenna. Although the form factor of the IC-905

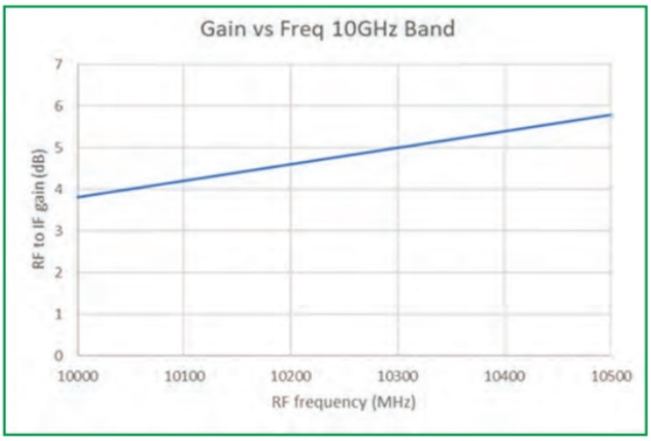

FIGURE 2: The gain over the whole 10GHz band from 10000MHz to 10500MHz.

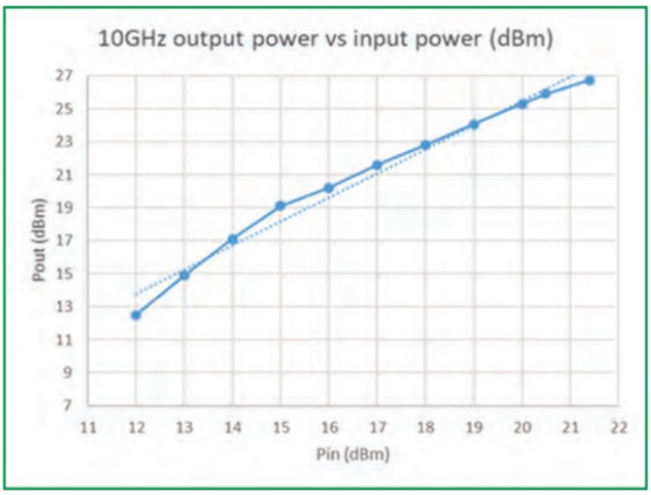

FIGURE 3: Transverter output power vs input power at 10368MHz.

FIGURE 4: A screenshot showing both transmit and received pictures.

Table 1: Measured current consumption in Amperes on FM or ATV.

	Current consumption (A)			
	12V		13.8V	
Band	Rx	Tx	Rx	Tx
144MHz	2.2	4.4	1.9	3.8
432MHz	2.2	5.1	1.9	4.2
1296MHz	2.5	5.8	2.1	4.7
2400MHz	2.7	3.5	2.4	3.0
5600MHz	2.8	3.8	2.4	3.3
10368MHz	3.2	4.2	2.7	3.5

controller is the same as that of an IC-705, it is quite different in operation. Firstly, it needs to be connected to the external RF unit, where all the RF connections are made, and secondly it has no internal battery; it needs an external 13.8V supply. We observed that the controller's rear heat sink gets quite hot. It's perhaps not suited to use inside the same sort of temporary protective bag as has proved popular for the IC-705 when 'out portable'.

Power supply

The IC-905 is specified to function on 13.8V +/- 15%. As the unit includes an internal switch-mode power supply, there is no variation in power output over this range, a very useful feature if operating from batteries. In some example tests, the receiver stopped working below about 10.5V, and the transmitter stopped working below 11.4V. This is impressive performance, but it would have been good to have some sort of 'low battery' warning on the screen before the rig went dead. The current consumption was measured on each band at two input voltages and is shown in **Table 1**.

Connection of the 10GHz transverter did not appreciably increase the current consumption on the lower bands. With a 12V supply, the transmit current consumption can be as high as 5.8A; however, the standard OPC-2421 DC power cable (as also used on the IC-705) is supplied with 8A fuses. Note that the cable for the IC-705 contains 4A fuses which will blow with this radio! The 2.5/5.1mm barrel type of power connector employed on the controller is normally only rated to 5A, but the type fitted did not seem to get too hot during operation.

SD card

The IC-905 includes the very-useful facility of being able to save settings, data, voice, pictures, and screenshots on an SD card. The card slot accepts a full-size SD card, not the more common micro-SD card as used, for example, in the Raspberry Pi. The IC-905 software includes a 'Format' function, but it was found that this did not format the card in the usual sense; it simply wrote the folders required for IC-905 operation into an existing FAT32 partition. If the card was not already formatted with an FAT32 partition, the IC-905 'Format' command failed.

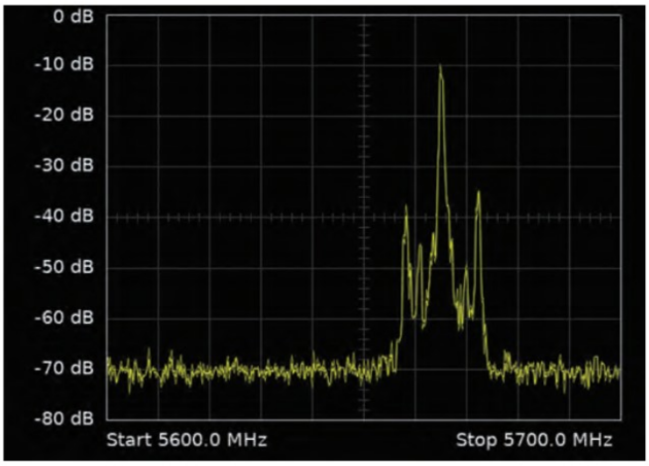

FIGURE 5: IC905 FM ATV spectrum.

Cable to the RF unit

The RF unit is connected to the controller by a screened 8-core cable with screened RJ-45 connectors. The supplied 5m cable is made from screened Cat 5e 24 AWG stranded cable. The conductor resistance was measured to be about 0.3Ω for each core, and it used standard straight-through pin mapping. The connection at the RF unit end uses a water-resistant connector with an internal RJ-45 connector by ODS-tech; this is on a short flying lead from the bottom of the RF unit. Given that the lead type and connectors are commercially available, there appears to be no reason why users could not make up their own cables to connect the RF unit to the controller. Although all the signals are digital with 'Power-Over-Ethernet', it is very unlikely that the connection could be made through an existing LAN connected to other devices.

RF unit water resistance

The specification does not make any claims for the water resistance of the RF unit. Worryingly, it is fitted with connectors both on the top and on the base of the unit. The companion 10GHz transverter (the CX-10G) specifies IP55, and it has all the connectors on the base of the unit. Given the value of this equipment, it would seem advisable to put the RF unit in a waterproof enclosure (with reasonable ventilation or cooling to dissipate the heat generated), or at least to make sure that all the connectors were sealed with self-amalgamating tape or similar to protect the unit from the UK weather.

Frequency locking

The RF unit includes a GPS receiver which can be used to stabilise the internal frequency reference, and can also be used to determine your location. The antenna input provides 3.3V, and so works with most commonly-available GPS antennas. A 10MHz output is available from the RF unit to feed the optional 10GHz transverter. There is no facility to feed in an external, existing, frequency reference to the RF unit – GPS is the only option. The 10GHz unit will not function without the 10MHz reference input.

John Worsnop, G4BAO
john@g4bao.com
Dave Crump, G8GKQ
dave.g8gkq@gmail.com

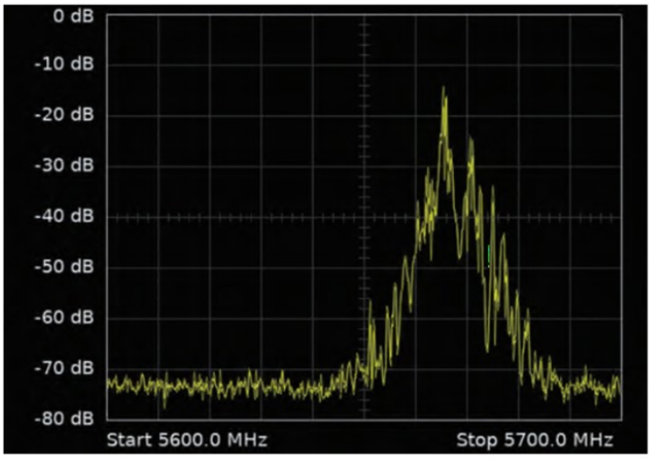

FIGURE 6: Drone Tx FM ATV spectrum for comparison.

PTT switching

The 3.5mm 'send' jack on the left side of the controller can be used to key the IC-905 to transmit by grounding the tip. Additionally, the tip is pulled from about 3.3V to ground when the unit is keyed to transmit by the fist microphone PTT button, or by the VOX. There is no provision for switching of external PAs or preamps by a DC voltage on any of the antenna connections. This has proved to be a popular after-market modification to the IC-705, so it is surprising that it has not been incorporated into the IC-905.

Performance testing: narrowband receiver operation 144MHz to 5.7GHz

Sensitivity measurements

No measurement of sensitivity was done at 5.7GHz due to lack of a suitable signal generator, but tests with a 5dB excess noise ratio (ENR) noise source indicated that sensitivity was adequate. As no access was available to the IF, no noise figure measurements were made below 10GHz.

For the other bands, sensitivity in SSB mode was measured as the RF input level in dBm to produce an audio signal-plus-noise to noise ratio of 3dB, rather than the method of 12dB signal-to-noise and distortion ratio (SINAD) used by the manufacturer. Our method gives a better measure of the threshold SSB and CW weak-signal performance, and will produce a correspondingly-lower signal than the result for 12dB SINAD. Using a true RMS voltmeter, the audio level was first measured with no input signal to the receiver. A signal was then injected to produce a 1kHz audio tone and increased until the audio output power increased by 3dB. This is an RMS voltage increase of a factor of 1.414. The results are shown in **Table 2** along with the level required to show 'S9' on the bar-graph S-meter. The standard definition for S9 at VHF and above is -93dBm.

Note: the manufacturer's sensitivity for 12dB SINAD (at 144MHz) is given as -6dBμV emf. This emf (0.5μV), from a 50Ω source, will develop 0.25μV across a 50Ω load (the receiver input), corresponding to an input power of -119dBm. The threshold measurement for 3dB signal-to-noise ratio made in this review was -135dBm.

Table 2: Receiver threshold sensitivity for +3 dB (S+N)/N

Frequency (MHz)	Threshold sensitivity (dBm)	Signal level for 'S9' (dBm)
145	-135	-92
432	-137	-92
1296	-134	-90
2320	-133	-91

FIGURE 7: The IC-905 received picture captured on an external recorder.

Transmit power output

At full output, the IC-905 has a remarkably-flat power output versus frequency curve. With output set to 100%, RF power is flat to within 0.5dB over the full tuning range, and easily met the specified output power on all bands (**Table 3**).

Transmitter harmonics

The transmitter's harmonic spectrum was measured on each band using a spectrum analyser, but no fundamental notch filter. The fundamental power to the analyser was carefully controlled to avoid overload, allowing levels down to -60dBc (dB down on fundamental carrier) to be measured.

No harmonics or other spurious emissions above -60dBc up to 24GHz could be seen with this test setup. This met or exceeded the manufacturer's specifications of a worst-case out-of-band emission of -43dBc in the 2400MHz and 5600MHz bands.

Performance testing: the CX-10G 10GHz transverter

Noise figure and gain

The 10GHz transverter unit has a wide bandwidth, covering from 10000MHz to 10500MHz. It seems to achieve this by changing its local-oscillator frequency, allowing the wide band to be covered seamlessly in sub bands of 50MHz width. As this part of the review focuses on the narrowband SSB/CW and digital modes, the main measurements were made in the European 10386MHz band. The transverter lends itself to a conventional RF-to-IF noise-figure measurement using a down-converter to bring the transverter's IF into the range below 1500MHz that an HP 8970 noise-figure test set can measure. The total noise figure of the transverter was measured using a 15dB ENR noise source, and an SG Lab 2.4GHz transverter to convert the IF to 432MHz. The SG lab transverter, used as a down converter, had a gain and a noise figure of 12.7dB and 2.3dB respectively. The gain and noise figure of this arrangement, including the down-converter, was 17.5dB and 5.5dB respectively.

Using standard cascade noise-figure and gain calculations [2], the 10GHz transverter's individual gain is calculated to be 5dB, and the noise figure 5.5dB. This is as expected with the manufacturer quoting '6dB typical' for conversion gain. Using the VK3UM receiver-performance calculator, this noise figure corresponded to a minimum detectable signal level (MDS) of -136dBm. This agrees with the manufacturer's specification of -17dBμV or -124dBm for 10dB signal-to-noise ratio.

Typical late-20th century 10GHz transverters of the sort used by many GHz-

Table 3: Manufacturer's power output specification.

Band (MHz)	Mode	Power (W)
144/430/1200	SSB, CW, FM, RTTY, DV	10
144/430/1200	AM	2.5
2400/5600	SSB, CW, FM, RTTY, DV	2
2400/5600	AM	0.5
10000	SSB, CW, FM, RTTY, DV	0.5
10000	AM	0.125

FIGURE 8: QO-100 testing with a 1.2m dish for Tx, and a smaller dish for Rx.

band enthusiasts have gains of 15dB and noise figures of 2dB. These would be 6dB more sensitive than the IC-905. This disappointing result means that, for serious weak-signal work, a mast-head preamp and associated sequencing will be essential when using the IC-905 on the 10GHz band.

Receiver gain flatness

The input signal was swept from 10000MHz to 10500MHz and the RF-IF level recorded (see **Figure 2**). It showed that maximum gain was at 10500MHz falling smoothly by 2dB at 10000MHz.

Transmit power output as a function of frequency

At full output, the transverter again has a remarkably-flat power output as a function of frequency. With output set to 100%, RF power is flat to within 0.5dB over the full tuning range, and easily meets the specified output power on 10GHz (**Table 3**).

Transverter harmonics

The transverter harmonic spectrum was measured using the same method used for the main transceiver. No spurious emissions or harmonics were seen up to 24GHz.

Transverter linearity

Linearity is usually measured by injecting two closely-spaced RF carriers into the IF input of the transverter, and measuring the power of 3rd-order inter-modulation products on the output. This can be done by resistively combining two RF carriers, or using an SSB transmitter with two-tone modulation. Because of the difficulty in getting a linear RF source at 2.4GHz (and the fact that only one good signal generator was available), a two-tone inter-modulation test was not carried out on the transverter alone. However, some measure of linearity can be made by plotting the transverter's output power versus input power curve, and measuring the 1dB compression point P_{1dB}. The higher the value of P_{1dB} the more linear the transverter. This test was carried out instead by using a power meter and a directional coupler on the input to the transverter, and a second power meter on the output. **Figure 3** show the results. Saturated CW power of the transverter was around +27dBm (0.5W) with little or no compression. This compares well with the manufacturer's specification of 0.5W, and indicates that the transverter is linear up to full-rated power.

Table 4: Comparison with other FM TV sources.

Equipment	Deviation at crossover	Pre-emphasis	Audio
IC-905	5MHz/V	Yes - unknown	Nil, 4.5, 6 or 6.5MHz
BATC 23cm	8MHz/V	CCIR 405-1 (625)	6MHz
Drone 5.6GHz	16MHz/V	None	6MHz and 6.5MHz

Performance testing: amateur TV operation

One of the headline features of the IC-905 is that it includes an amateur TV mode. On 1296MHz, 2400MHz, 5600MHz, and 10GHz (if fitted), it will transmit and receive frequency-modulated ATV pictures with a single sound sub-carrier. Over the last 20 years in the UK, this mode has gradually been replaced by digital DVB-S/S2.

Connecting a camera

TV transmission requires a PAL video camera to be connected to provide the picture source; this can be an old camcorder, or a more-modern alternative, such as the BATC PAL Video Source **[3]** using a Raspberry Pi camera. The audio can be from the fist microphone or from an external mono audio source. The required leads are not supplied, but they can easily be made up from a 3.5mm stereo jack plug; although the manual indicates that a 4-terminal jack is required, the ring furthest from the tip is not connected, so a standard 3-terminal stereo jack will suffice. The transmitted picture can be shown alongside the received picture on the touchscreen (see **Figures 4 and Figure 7**); either picture can be enlarged to full screen simply by touching it. An external monitor can be connected to display (or record) the received pictures.

Frequency modulation

The TV modulation standard is not specified in any of the Icom documentation we have seen so far. The FM ATV deviation was measured to be significantly lower than has traditionally been used for ATV in the past. Pre-emphasis is also applied in the transmitter (with matching de-emphasis in the receiver), but the exact pre-emphasis standard is not stated by Icom. The parameters are compared to those commonly used in the **Table 4**.

The FM ATV modulation appears to be generated in software and, with the low deviation, gives a tight (for FM ATV) ATV spectrum of about 14MHz wide. The spectrum is compared with that from a 5.6GHz drone transmitter in **Figure 5** and **Figure 6**. The occupied bandwidth of 14MHz is approximately 30 times that occupied by a digital ATV transmitter carrying the same (or better) quality signal in just under 500kHz. Not only does this have spectrum-occupancy implications, but it also increases the signal power required to make a TV contact by a similar amount.

On-air testing and compatibility

Initial on-air tests were conducted between a pair of IC-905s on 5665MHz. The received picture quality was about P4 (over a 29km line-of-sight path) with one station using the Icom AH-56 5dBi collinear-array antenna and the other using a 22dBi ex-WiFi dish. The audio was clear, with the welcome facility of an FM squelch on the audio subcarrier.

A few ATV repeaters still retain an FM receive capability. Initial tests transmitting into GB3SQ over a distance of 11km were successful, but the picture quality was poor as it was set up for the more-commonly-used deviation of 8MHz/V. The repeater keeper, Colin, G4KLB, then installed a video AGC system, and further tests a week later gave better results. It is likely that most UK ATV repeaters would need similar modifications to receive ATV transmissions from the IC-905.

The IC-905 showed significant crushing and tearing of the video when receiving signals from an unmodified 1255MHz transmitter. There is no facility on the IC-905 to accommodate the wider deviation that causes this, so any such transmitter (or remaining repeaters transmitting FM ATV) would be incompatible with the IC-905 without modification.

Tests were also conducted on 5665MHz, investigating compatibility with the popular (and cheap) drone transmitters and receivers. Tests were successful after significant modifications to the drone equipment. On transmit, the drone transmitter video level needed reducing, and pre-emphasis needed to be applied. Some patterning from the high level of the two sound sub-carriers remained visible on the IC-905, but the results were acceptable. On receive, significant amplification of the video signal was required, and it

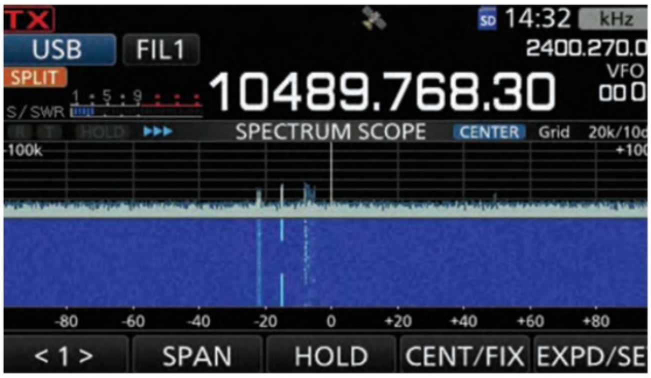

FIGURE 9: QO-100 receive spectrum scope.

needed de-emphasis to be applied. Full details of these modifications will be published in the BATC's CQ-TV magazine in due course.

Digital ATV

The IC-905 only transmits and receives analogue FM ATV. It is a shame that no attempt has been made to handle DVB-S2 digital ATV which is now the predominant ATV mode in the UK and on the QO-100 satellite. As the unit has no 'IF' input or output, the only likely option for introducing this capability would be an internal firmware upgrade.Unfortunately, it is unlikely that the internal processor could handle the challenging error-correction processing required for reception, as this is usually handled in custom integrated circuits. The omission of digital ATV might preclude the use of this rig for any ATV operation in the 1296MHz band following the possible future implementation of restrictions to safeguard radio-navigation satellite services (RNSS).

Further on-air tests

Due to the limited time available and the authors' lack of familiarity with digital voice operation, just a few on-air tests were made.

FM voice repeater operation

The radio was tried on three local repeaters, GB3PI (2m), GB3PY (70cm) and GB3PS (23cm). It was simple to set up the sub tones and shifts from the menus with reference to the manual, and good audio reports were had on all bands. It was easy to access GB3PS on 23cm with just 100mW (1% power level) and a three-element PCB Yagi antenna in the loft at a line-of-sight range of 32km.

D-Star operation

The radio has extensive D-Star facilities, both data and voice, but the reviewers have to admit that (as GHz bands and ATV specialists respectively), they're quite unfamiliar with DV radio. However, with help from **[4]** the reviewers did manage to set up the radio to access a local 70cm D-Star repeater (GB7PI), and it was straightforward to do that from the menus.

QO-100 SSB operation

The IC-905's 2W output on 2400MHz SSB is sufficient to access the QO-100 narrowband transponder if a 1.2m dish is used (see **Figure 8**). The receiver in the CX-10G transverter is just sensitive enough to receive the output of the narrowband transponder on 10489.5MHz, but benefits from an external preamp as mentioned in the measurements section on the 10GHz transverter. Careful consideration needs to be given to the configuration of any QO-100 installation. Cable losses between the 10GHz receive feed, and the 10GHz transverter (or the use of a smaller dish), normally necessitate a receive preamp mounted at the feed. Cable losses on transmit at 2.4GHz can also be significant.

The spectrum scope on QO-100 (**Figure 9**) was useful, but it was frustrating that, although split-frequency operation between 2.4GHz and 10GHz was easy to set up, there was no duplex capability, so the spectrum scope was not visible whilst transmitting. As the 10GHz transverter uses the 2.4GHz band as IF, full duplex on QO-100 is not possible. If internet connectivity is available, the QO-100 narrowband WebSDR **[5]** could be used to monitor the transponder during transmit. It would be useful to set the (2.4GHz) transmitted frequency to track the (10.49GHz) received frequency as it is tuned across the transponder. However, it did not seem possible to set the 8089.5MHz offset required, which made netting to received stations awkward. Hopefully this can be added as a new feature in a future firmware update. This capability may be available if the radio is tuned using an external computer program.

Conclusions

The IC-905 is a capable VHF/UHF/SHF CW/SSB/FM transceiver, and is great for someone who wants to get a feel for the microwave bands, or set up dedicated 'plug and play' backbone networks such as might be used by Raynet and similar organisations. The remote RF unit and transverter tackles the issue that all GHz and homebrewers have solved with varying success over the years, namely that of reducing feeder losses between the antenna and the radio, and operating it all in an outdoor environment.

In some ways, the rig is a bit of a game changer, but in our opinion it has not been aimed at existing GHz-band specialists in Europe. Most European GHz contest, or DX operation, is either done 'off grid' on hilltops with portable equipment requiring low power consumption, or with optimised home systems. Especially on 10GHz, better performance can be had at the price with a more-conventional radio and individual transverters. However, the rig does minimise the engineering skills needed to operate on the GHz bands both in RF system design and the mechanical engineering of operating equipment outdoors and off-grid. This has to be a good thing if it generates more activity on the bands above 1GHz. That said, using it with suitable preamps (for 10GHz) and horizontally-polarised dishes or panel antennas, will produce very good results with few of the engineering skills needed to make SHF QSOs using assorted system modules.

Finally, it's unfortunate that the rig has limited ATV compatibility with other equipment used in Europe; specifically, there is no means of using it for digital ATV. In the 21st Century, and certainly in Europe, this is a *de facto* standard for ATV. We both agree that this would be a welcome addition to the product. It may be that, as much of the capability is in software, Icom may be able to include the transmission of DATV in future releases of the product, but G8GKQ's view is that there is currently not sufficient processing power to manage reception with the existing hardware.

Acknowledgements

Our thanks go to Sam, G4DDK, for suggesting and helping with some of the measurements made in this article, and to Icom UK's Ian Lockyer for providing the test samples.

References

[1] Download the basic user manual at: https://www.icomjapan.com/support/manual/3762/
[2] Cascade noise figure: https://tinyurl.com/mvcdwuwz
[3] https://wiki.batc.org.uk/BATC_Video_Source
[4] http://www.dstarinfo.com/home.aspx
[5] https://eshail.batc.org.uk/nb/

You can watch Bob McCreadie, G0FGX, Dave Crump, G8GKQ and Noel Matthews, G8GTZ putting the IC-905 through its paces on Episode 29 of TX Factor. During testing, the team made FM voice QSOs on the 5.7GHz band and exchanged ATV images. Following this they used the optional 10GHz transverter and made SSB QSOs.
TX Factor is sponsored by the RSGB.
Find the latest episode at txfactor.co.uk

A digital Hobbs meter for amateur radio

Who is Hobbs, and why do we need a digital version of his meter? The story of the Hobbs meter began during the second world war in the aeronautical industry, specifically in aircraft maintenance.

Introduction

Since the amount of ground covered by an airplane could vary a great deal (even with the engine running at a constant speed), because of the effects of a tail-wind pushing the aircraft forward or head-wind increasing the resistance to forward motion, aircraft engineers had to find a method to gauge when the aircraft needed maintenance other than by estimating miles travelled. John Weston Hobbs (1889-1968) came up with a meter that would count hours of operation based upon the rotational speed of the engine, and this meter was named after the inventor (see **Figure 1**).

So how does this connect to amateur radio? There are several circumstances in which keeping track of hours of operation is useful. This goes beyond technical issues such as trying to gauge when a thermionic valve may go soft near the end of its operating life; it also embraces non-technical aspects such as keeping track of public-service operations, how long you have been on the air, etc. With a bit of consideration, you can think of plenty of other examples where keeping track of time would be useful.

No doubt the Civil Aviation Authority would take a dim view of us requisitioning a Hobbs meter from an actual aircraft, so let us instead take a look at how to put one together ourselves, including a way to make this device a bit more modern in the process. Figure 1 shows an actual Hobbs meter (this one manufactured by Motorola). In this project, we will upgrade the concept to go from a mechanical device, such as that shown in the figure, to a digital electronic device which has a numerical LED display.

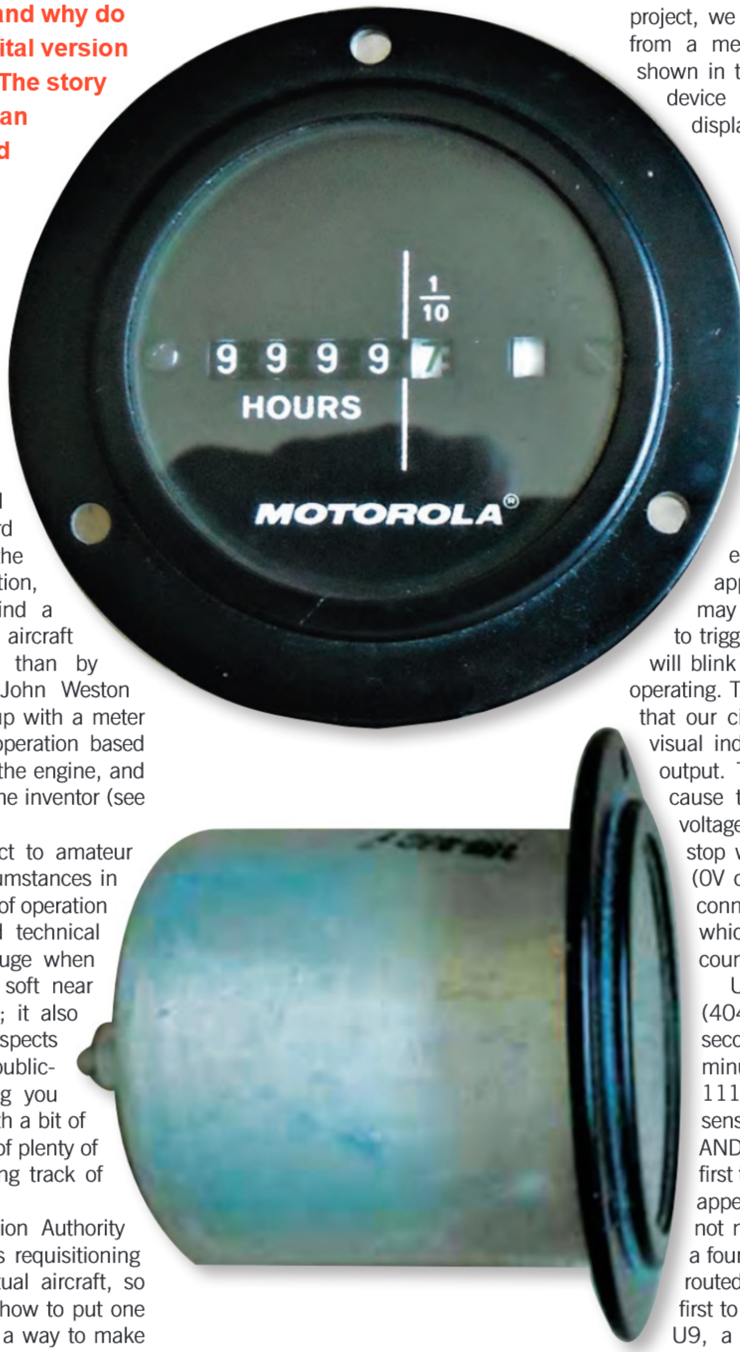

FIGURE 1: **An aircraft Hobbs meter: above front view and below side view.**

How the circuit operates

The circuit diagram of the digital Hobbs meter is shown in **Figure 2**. A 555 timer (U1) is wired to run at 1Hz in order to keep components reasonable in value and cost. Resistors R1 and R2 should have the same value, or at least be close, in order to keep the output waveform close to symmetrical. As they become more and more dissimilar from each other, the output voltage approaches a periodic spike. This may cause the counters downstream to trigger unreliably. LED 1 and LED 2 will blink (alternately) when the circuit is operating. These LEDs will indicate not only that our circuit is active, but also give a visual indication of the symmetry of the output. The "RESET" input (pin 4) will cause the 555 to oscillate when the voltage is set to a logic "1" (+12V) and stop when it is held low at logic "0" (0V or ground). The output of U1 is connected to a CMOS counter (U3) which therefore counts at a rate of 1 count per second.

U3 is a 12-bit binary counter (4040) which counts up to 3600 seconds (60 seconds/minute x 60 minutes/hour), which is a binary 111000010000. This count is sensed by U6A, half of a dual 4-input AND gate (note that this count is the first time that these particular four 1s appear in the count from zero, so it is not necessary to use any more than a four-input AND gate). This output is routed down two separate paths: the first to the clock inputs of U4, U7 and U9, a chain of 14510 binary-coded decimal (BCD) counters, and second to U6B, used here as a 2-input AND gate.

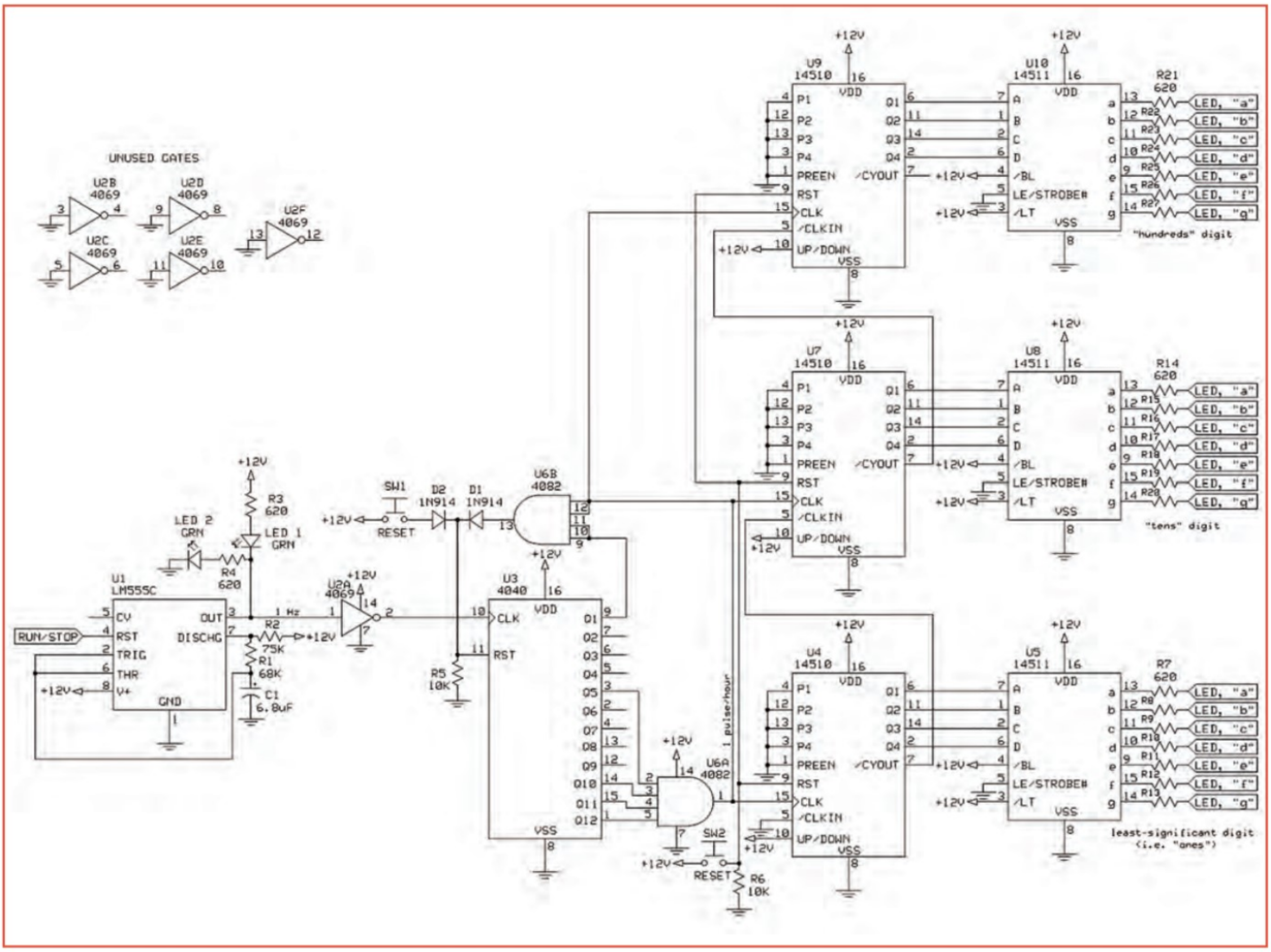

FIGURE 2: The circuit diagram of the digital Hobbs meter.

When U6B sees a count of one hour plus one second, it provides a reset pulse to U3 (it should be noted here that the 4040 operates in the opposite sense to the 555 in that it is enabled to count when the "RESET" input is held low). D1 and D2 act as an OR gate so that either the circuit can reset itself to zero, or the operator can cause a reset via SW1, a momentary normally-open switch. SW1 can be used in case the user needs to reset the count to zero manually. The 4040 will be at a count of zero every time it is powered up (as most, if not all, logic gates do).

The difference between a binary counter and a BCD counter is that a binary counter, like the 4040, will start at zero and keep counting up in binary, whereas the BCD counter, like the 14510, resets itself internally after ten counts, so acts as a base-ten counter instead of as base-16 counter. The "overflow" from U4, as count 9 goes to count zero, is fed to the next BCD counter in the chain U7, and the overflow from U7 is fed to U9. These three BCD counters therefore count the units, tens and hundreds of a three-digit decimal number. Figure 2 shows enough counters and displays for 999 hours, but you can add additional BCD counters to the chain if you need to go beyond this.

The LED displays

The four-bit outputs of each BCD counter are connected to the four inputs of respective BCD to 7-segment decoder drivers U5, U8 and U10. These 14511 chips interpret the binary inputs so as to light up the correct segments of 7-segment LED displays. There are no specific part numbers specified for the numeric displays themselves since these are not critical; several different physical sizes and colours exist making the choice of which to use dependent on the user's preference. The only critical thing to watch out for is whether the display is common-anode or common-cathode since each requires different wiring. Check the data sheets for the LED driver ICs and LEDs for proper wiring. I show wiring for both types in **Figure 3**.

Operation

Since the integrated circuits we are using do not have any memory capabilities, the count (and display) will return to zero once the power is disconnected. Therefore, some type of back-up power is needed for long-term use, as shown also in Figure 3. On-board batteries are suggested to prevent accidental disconnection. The secondary power source, in the case of batteries, needs to be monitored so that if they become drained they need to be replaced in a timely fashion. Also, since the LED displays require a lot of current

Klaus Spies, WB9YBM
wb9ybm1@yahoo.com

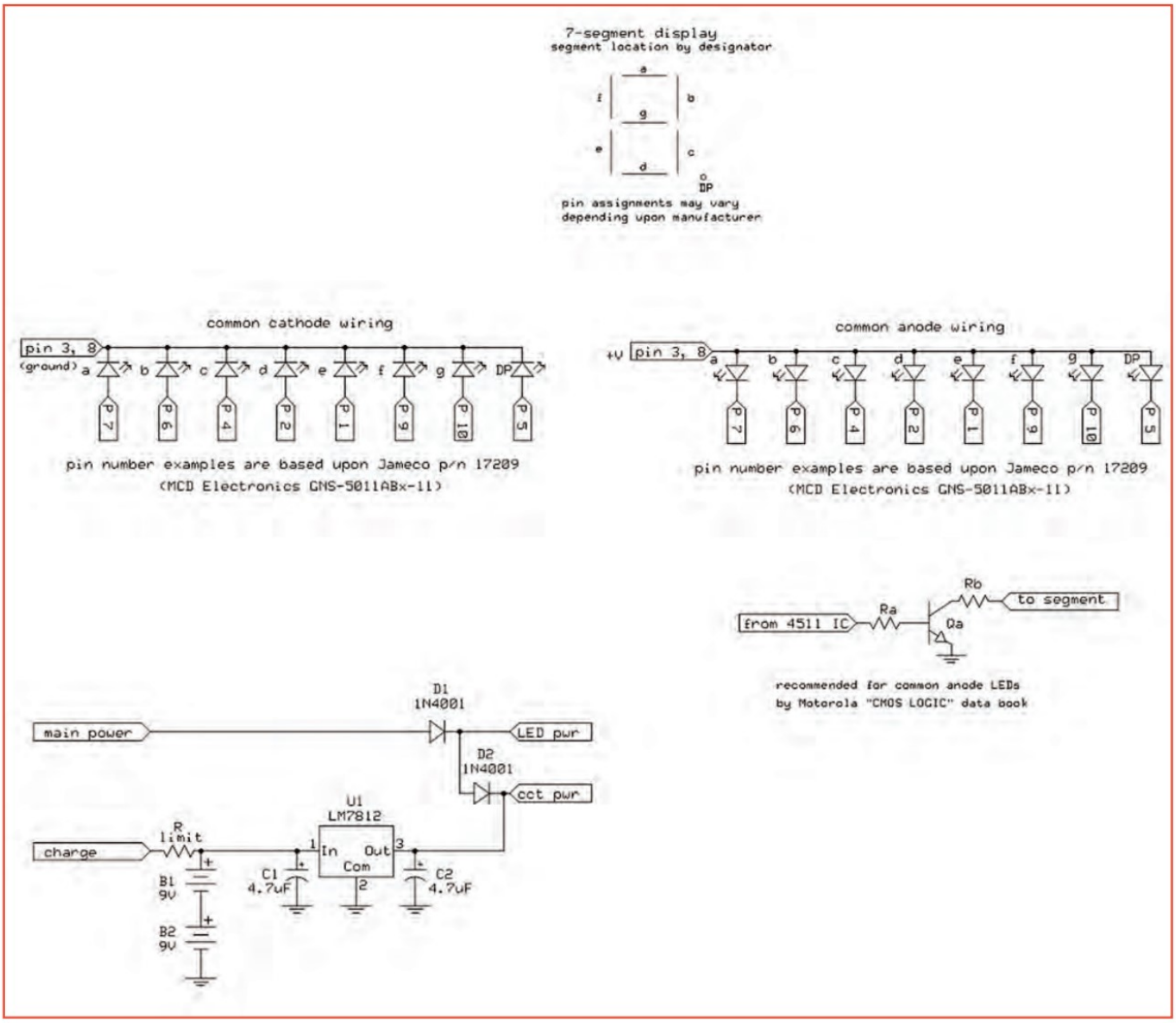

FIGURE 3: Common-anode and common-cathode LED display wiring, and back-up power supply wiring.

relative to the integrated circuits, they are disabled when the primary power is turned off. You may also like to consider connecting the +12V supply to LEDs 1 and 2 instead to the "LED pwr" line, so saving a further 15mA or so of current drain. Note, however, that in this case there will no indication that your Hobbs meter is actually doing anything. The circuit shown in Figure 3 also provides for the re-charging of the batteries, if desired. The re-charge option can be omitted if a secondary power source is chosen that does not involve batteries. Re-set switches are included in Figure 2 in the event that a manual re-set is desired (it may be needed in certain applications – after all, we haven't explored *everything* that this circuit can be used for).

Construction

This circuit does not have any medium- or high-impedance connections that would make it susceptible to picking up stray RF, nor does it have any fast digital signals that could 'spray' into adjacent circuitry. Therefore, no special shielding or metal enclosure is needed, although of course some kind of enclosure is still recommended to protect the circuitry from the outside world as well as giving it a neat, professional appearance. The primary reason I would recommend a metal enclosure is because of the LEDs: depending on how many are used, current requirements can be a concern. If we install an on-board power supply, a metal enclosure would provide a heat-sink for the regulator.

Extras

The 1Hz signal from the 555 timer can also be fed to a decimal point of one or more of the digits (if the numerical displays we choose are so equipped, as most are). This will not only indicate that the circuit is functioning but will also make the display look a bit more interesting.

Conclusion

This project not only provides us with a unique piece of equipment for our shacks but can also be used in other applications, such as making sure the kids don't go overboard playing video games! Of course, there's also the 'wow!' factor when a guest or visitor sees blinking lights!

Technical

dsPic-based audio processor

for driving quadrature RF up-converters using the direct or Weaver mode

Anyone building a direct up-conversion transmitter needs to generate a pair of quadrature, or I/Q, audio channels with a fixed 90° phase shift between them over the entire frequency band of interest.

Traditionally, this has been done with either a polyphase network, or several (usually six) op-amps arranged as all-pass filters. As an alternative, the so-called 'third method', or Weaver technique, is used in which the base-band audio input is mixed down in a pair of 90°-shifted LO signals at typically 1800Hz so it is folded around its centre frequency. The complete spectrum is then reconstituted, or unfolded, in the subsequent conversion to RF. The unit described here employs digital signal processing to perform either a 0/90° conversion, or a Weaver conversion. In addition, Tx/Rx switching using audio-triggered voice-operated transmit (VOX) is provided, together with two LEDs for optimising audio drive levels.

Overview

The unit described takes in audio signals from a microphone amplifier, a PC sound card, or from any other source that is intended to drive a transmitter. The dsPic chip's internal analogue-digital converter (ADC) samples the incoming audio, filters it to speech bandwidth, and converts to a pair of 90°-shifted base-band waveforms for driving a quadrature RF up-converter. Two converter modes can be selected, either direct up-conversion with no frequency translation, or Weaver mode. In the latter, the audio is first down-converted about its centre frequency to form a pair of overlapping quadrature channels of half the

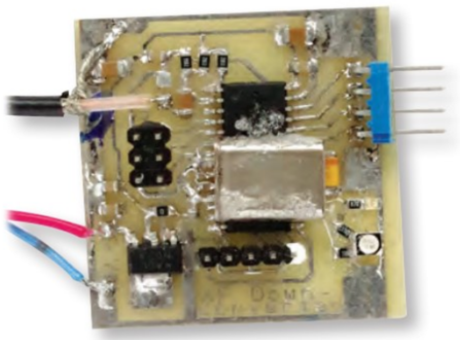

FIGURE 2: The bread-board PCB used for dsPic firmware development.

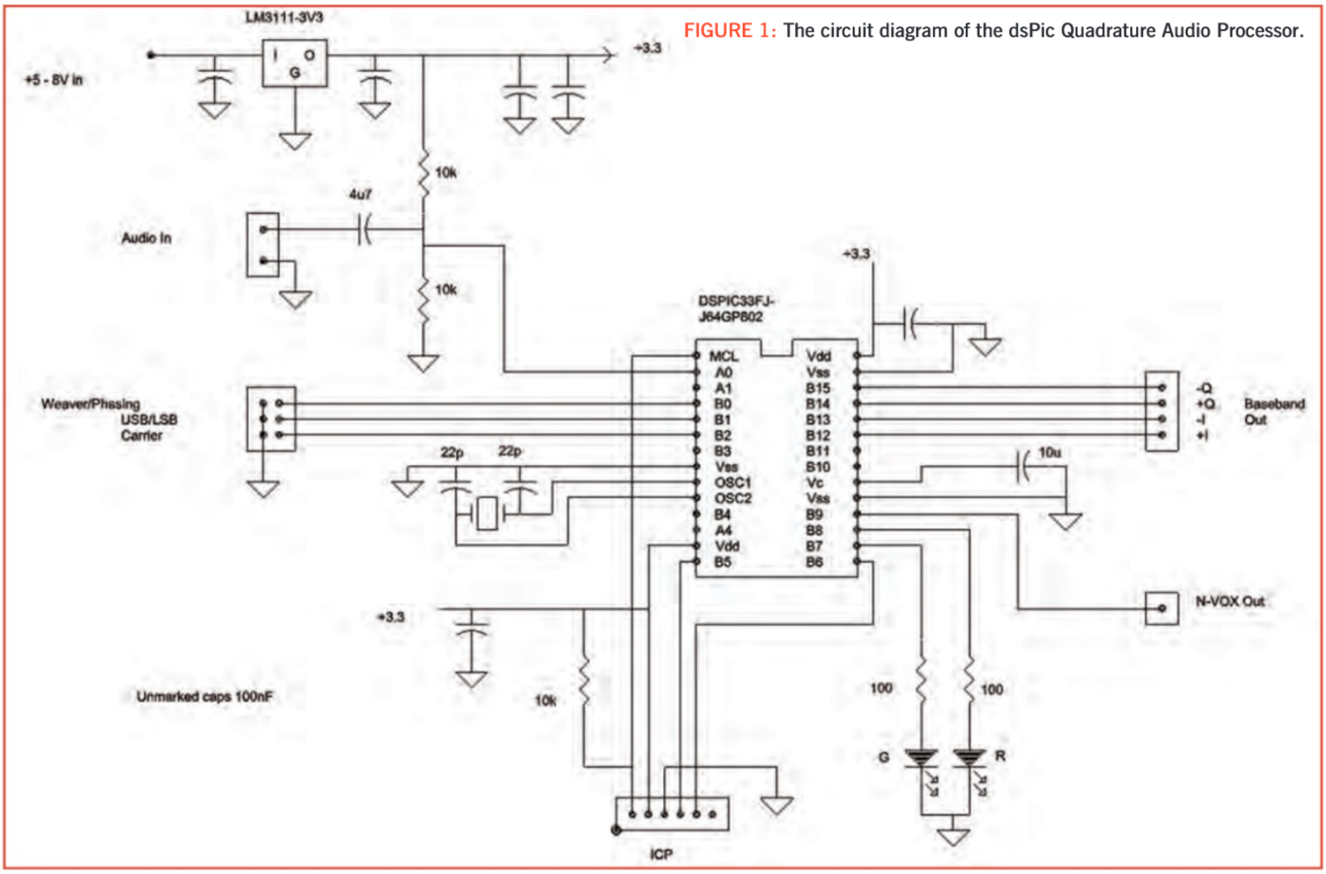

FIGURE 1: The circuit diagram of the dsPic Quadrature Audio Processor.

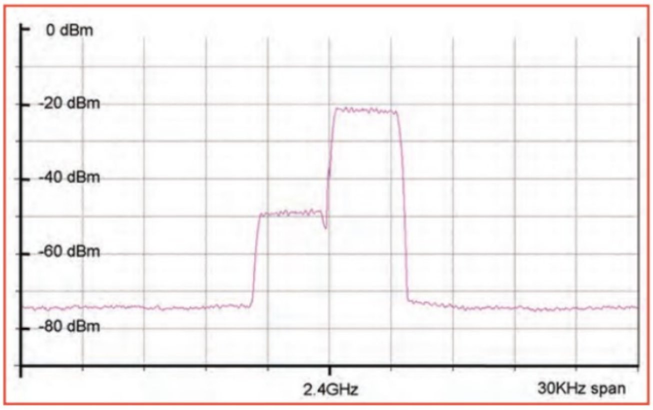

FIGURE 3(A): Broadband noise converted using USB direct conversion.

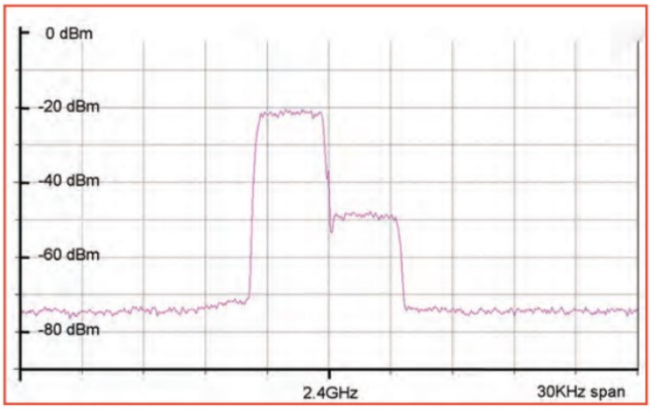

FIGURE 3(B): Broadband noise converted using LSB direct conversion.

input bandwidth, which are low-pass filtered and sent to the on-chip output digital-analogue converters (DACs). The two overlapping side-bands are reconstructed in the subsequent RF up-conversion. Weaver and direct up-conversion each have their own advantages and disadvantages, so it is desirable to have the ability to choose the most appropriate mode, and to be able to seamlessly switch between them.

Upper or lower side-band conversion is user-selectable, and another option allows a DC level to be added to the output to give a plain carrier output for testing and calibration purposes. For help with adjusting the input level during operation, two level-setting LED indicators are provided. A green LED flashes with drive level when this is within the optimum range for the converter, while a red one illuminates when input overdrive is approached. A VOX output with hang-delay is provided for controlling a transmitter, activating a logic line when the audio input exceeds a certain level.

DSP functionality

The first-generation code adopted an audio sampling rate of 27.2kHz. The input sample stream is first filtered in a 201-tap finite-impulse response (FIR) band-pass filter (BPF) covering 100Hz to 3400Hz. The low-frequency cut-off is needed to remove DC bias in the input analogue circuitry driving the ADC. If direct conversion is in use, rather than Weaver, the audio samples are then applied to a FIR phasing network that applies a +/- 45° phase-shift to each channel. The two resulting 90° phase-shifted I/Q outputs go directly to the output DACs.

For Weaver conversion, the band-pass filtered ADC samples are applied to a pair of mixers driven by a numerically-controlled oscillator (NCO) running at 1700Hz. The mixer outputs are filtered in a 201-tap FIR low-pass filter with a 1700Hz cut-off; the I and Q outputs of the filters go to the output DACs.

For both types of conversion, a link connected to an I/O pin of the chip is monitored; if set low, the I/Q channels are swapped, changing the direction of the final RF up-conversion.

Background and updates

The first version was designed by Martin Farrell, G8ASG, who wrote all the DSP code. That version used the dsPic's internal RC oscillator and offered the two types of conversion with side-band selection. There was no capability to insert select-on-test values to apply a DC offset to the base-band outputs to optimise mixer balance for carrier and unwanted side-band rejection. The internal DACs on the dsPic do not have perfect DC balance, nor do most other mixer devices, so trimming to maximise the carrier rejection was unavailable.

The first modification defines two constants at the top of the software listing; these are added to the final DAC values from the DSP processing. By adjusting these constants, while using appropriate RF test equipment to monitor the output from the RF up-conversion, then re-compiling and re-programming the chip each time, a user can optimise the DC balance to get best carrier rejection. This is a simpler process than adjusting resistor values around extra analogue circuitry to achieve the same objective.

The original version of the firmware used the dsPic's RC-timed internal oscillator for a processor speed of around 35Mips, and was also used to generate the Weaver down-conversion with an NCO at 1700Hz for its centre frequency. Being RC timed, the frequency was only accurate to the chip's clock specification of 1%, and it could easily vary by a few hertz during operation. The firmware was modified for crystal control using a 7.3728MHz crystal; this was the same nominal frequency as the internal RC oscillator.

To give a bit more audio bandwidth, the audio sampling rate was raised to 28.8kHz, while keeping all the filter coefficients the same. This results in the input filter pass-band edges moving up in proportion to the increase in sampling rate, now 106Hz to 3600Hz, while the Weaver conversion frequency becomes 1800Hz with a corresponding rise in the output LPF cut-off frequency.

An extra connection to another pin on the dsPic, when grounded, replaces the DAC drive with a fixed value sent to both I and Q channels. This unbalances the mixers, allowing a plain carrier to be generated. The value is stored as a user-defined constant; currently this is set at a value that gives a peak carrier output 3dB down. Details of early versions of this design can be found at **[1]** and **[2]**.

On test it was subsequently noticed that, on modules where a reasonably-high value of DC offset was needed, the calculated 16-bit signed integer sent to the DAC was overflowing, delivering drive values of the wrong polarity that completely messed up the waveform, resulting in a wide-band highly-distorted RF signal. This was cured by checking for mathematical overflow after the addition of the offset constants, then forcing a default maximum or minimum. Output distortion when saturated in this way, while still present, is now at a considerably-lower level than if the value had remained uncorrected.

The final modifications, those for level-setting LEDs and VOX transmitter control, will be described later.

Andy Talbot, G4JNT
(original dsPIC code
by Martin Farrell, G8ASG)
andy.g4jnt@gmail.com

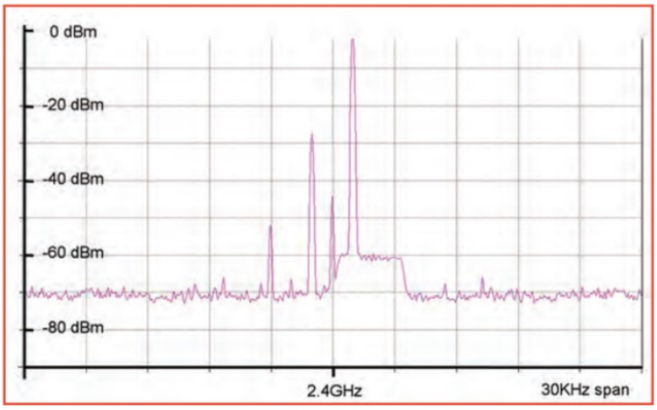

FIGURE 4(A): 1kHz tone direct conversion using USB.

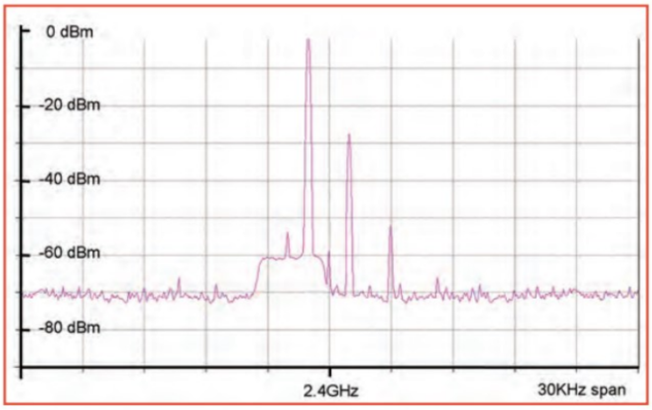

FIGURE 4(B): 1kHz tone direct conversion using LSB.

Weaver versus direct up-conversion

Direct quadrature up-conversion applies the input audio frequency band directly to the RF mixers. If upper side-band conversion is selected, the resulting RF frequency appears as the sum of the RF local-oscillator frequency and the audio frequency, at $f_{\mathrm{OUT}} = f_{\mathrm{C}} + f_{\mathrm{AUDIO}}$. The image at $f_{\mathrm{IMAGE}} = f_{\mathrm{C}} - f_{\mathrm{AUDIO}}$ is nominally cancelled by the quadrature up-conversion process, although this is never perfect when using real RF mixers. With careful select-on-test adjustment, the level can usually be reduced to better than -40dBc, sometimes a lot better, but this does need careful setting up and the use of high-stability components maintained at constant temperature. In some RF environments, this level of spurious image response, which may lie in an adjacent channel, can be unacceptable. One final imperfection is mixer imbalance, which results in carrier leakage that appears at the bottom of the translated frequency band, here 100Hz below the lowest wanted component.

In this event, Weaver conversion is more suitable. The 100Hz to 3600Hz audio input band is shifted down in frequency by the 1800Hz LO applied to the DSP mixers, to give a base-band output ranging from -1700Hz, through DC to +1800Hz. The spectrums of the upper and lower parts overlap, but are kept separate by the relative phase of their I and Q channels. The frequencies below zero have a 180° phase-shift compared with their corresponding components above zero, allowing reconstruction of the full spectrum in the quadrature up-conversion process.

Note that to get an identical frequency range output from direct and Weaver conversion, the RF local oscillator has to be set 1800Hz higher for Weaver than it does for direct conversion to compensate for the inherent 1800Hz down conversion in the DSP. For LSB conversion, the frequency offset needs to be in the opposite direction.

The unwanted, imperfectly-cancelled, converted side-band now lies, folded, on top of the wanted spectrum where it should not interfere with users on adjacent channels. For most digital signalling waveforms, an on-frequency interfering signal as bad as -15dBc causes little problem, so a rather poor side-band suppression of -20 to -30dBc is perfectly acceptable. Even the unwanted image from SSB speech converted using a Weaver approach, has been described as 'not particularly objectionable' at levels of -15dBc to -20dBc, appearing just as a weak high-pitched wrong-side-band interferer.

DC leakage is more of a problem with Weaver conversion. Since the base-band signal is a down-conversion by 1800Hz of the input audio spectrum, any DC imbalance in the mixer will now appear as if it had come from an 1800Hz component in the input; a real input at 1800Hz is converted to zero Hz. Again, for digital waveforms, this carrier leakage which can often be trimmed to a lower level than side-band cancellation offers, presents no problems at levels of -15dB or lower. But for voice signals, it appears as a constant frequency tone or whistle in the middle of the voice band, which can prove annoying.

Another disadvantage of Weaver conversion is that the frequency of the input signal is not maintained; it is shifted by an LO whose exact frequency is determined by the processor clock. If this is not itself generated from a high-stability source such as a crystal oscillator, or better, the resulting frequency-shift error can be unacceptable in high-stability RF links. This was observed when the dsPic's internal RC oscillator was used, leading to a few Hz error in the frequency conversion.

Hardware

The circuit diagram of the current design can be seen in **Figure 1** with a breadboard version on a first-generation PCB in **Figure 2**. This PCB was constructed for Martin's original version before the crystal timing and the level setting LEDs were added. The crystal, its associated capacitors, and the level-setting LEDs were wired directly to the IC pins.

The dsPic runs from a 3.3V supply rail that also provides the reference voltages for the A/D and D/A converters. The input is biased to half the supply voltage and is AC coupled, so therefore restricted to an absolute maximum of 3.3V peak to peak. The two DAC outputs are delivered differentially as plus/minus voltage outputs for each channel, sitting on a common-mode level of around 1.7V, broadly compatible with many quadrature up-conversion chips without the need for any extra analogue level conversion. One such device covering the UHF to low-microwave range is the ADL5375-1.5 whose data sheet can be found at **[3]**.

Level-setting LEDs and VOX transmitter control

The input A/D converter has 12-bit resolution so can potentially cope with an input dynamic range in excess of 60dB. However, to get best carrier rejection and lowest noise, the RF mixers need to run at close to their maximum specified input drive, so without incorporating some form of automatic gain control within the DSP code, input drive needs to be manually adjusted to achieve this condition whilst avoiding overload.

Two LEDs are connected to spare I/O lines. A green LED is used as a continuous monitor to ensure input audio exceeds a minimum threshold. First of all, the output from the ADC for every sample is squared to ensure positive and negative peaks are treated equally. The square-law characteristic also provides greater sensitivity than would a linear characteristic for peaks close to the maximum, making adjustment easier. When the instantaneous value of V_{in}^2 exceeds a user-defined threshold level, the green LED is illuminated. The threshold level is set at around 20dB below the input ADC saturation level,

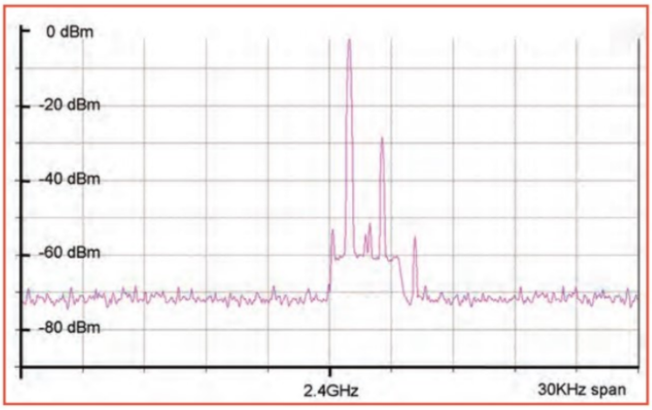

FIGURE 5(A): 1kHz tone converted using Weaver mode (USB).

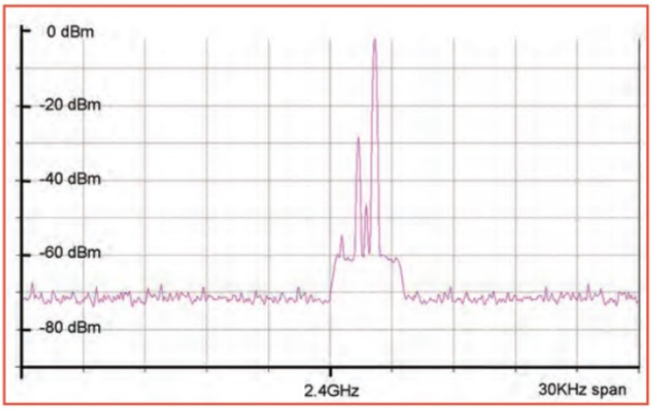

FIGURE 5(B): 2.2kHz tone converted using Weaver mode (USB).

meaning that the LED flashes dimly as the input level approaches the -20dB value, getting brighter as the input level rises. The idea is to keep audio input at a level that permanently illuminates the green LED.

Another threshold value is set, just below the point at which input clipping occurs, when the ADC output values start hitting their plus and minus limits. When the value of V_{in}^2 exceeds this upper threshold, the red LED is illuminated and stays on for 100 milliseconds, ensuring that even minor overloads are intercepted and shown. This is particularly useful when using speech, as occasional red peaks can be used for critical adjustment of the speech volume control.

A VOX output has been provided to activate a transmitter automatically when audio drive appears. The requirements for VOX operation are significantly more complex than the simple threshold detection used for the level-setting LEDs, and especially so when used for voice input. It needs to avoid being triggered by very-brief input pulses that may just be one or two samples in width caused by random noise or impulses, but must rapidly respond and stay activated when an input drive waveform with a strong amplitude component such as voice is applied. This is achieved using a rolling average of the input samples, using the algorithm:

$$V_A(t_i) = \frac{(N-1)}{N} V_A(t_{i-1}) + \frac{V_{in}(t_i)}{N}$$

where $V_A(t_i)$ is the running-average value of the input voltage after adding the current sample value of the input voltage, $V_{in}(t_i)$, N is a user-defined constant, and $V_A(t_{i-1})$ is the running-average value of the input voltage after adding the previous sample of the input voltage. The value of N is currently set at 200, allowing the average to build up over a period of this many samples. At a sampling rate of 28.8kHz, this is about 7ms, fast enough to follow syllabic speech and slow data waveforms like PSK31. When the average value exceeds an upper threshold, V_{VOXHI}, a counter running at the sample rate is started and the VOX output line is activated. The counter is then reset every time the average exceeds a lower threshold V_{VOXLO}, so with a continuous drive waveform the count rarely gets much higher than zero. When the mean drive level drops below the lower threshold long enough for the count to exceed a certain value, typically set for a 500ms delay, the VOX line is cleared. This use of two thresholds, in the same manner as a Schmitt trigger, minimises false triggering while also further helping to reduce dropouts during pauses in speech. The system appears to work reliably with speech that has no long pauses, with the 500ms hang time not giving an excessive delay on Tx/Rx switching for simplex communication using either voice or data.

Practical realisation: an S-band up-converter for the QO-100 satellite

The requirement was for an up-converter that could take in audio, either as speech or tones from a computer soundcard, and convert it to a frequency within the range 2400.5MHz to 2401.0MHz for the uplink to the QO-100 satellite narrowband transponder. It had to behave exactly as if it were a conventional SSB transmitter.

A similar dsPic module to that shown in Figure 2 was paired with an STQ2016 quadrature up-converter chip. This device covers the frequency range 700MHz to 2500MHz, and accepts differential I/Q drive using voltage levels that are compatible with the output from the dsPic DACs. In practice, the STQ2016 can accept a higher peak-peak differential drive voltage than the DACs can give, so the up-converter is not being driven to its maximum capability, and the RF output is about 6dB lower than it could be with full drive. The I and Q DAC offsets were adjusted for best carrier rejection with this particular combination of dsPic and up-converter, needing values for I and Q channels of -1100 and 1450 respectively, taking up an appreciable part of the -32768 / 32767 maximum levels permitted.

An LMX2541 fractional-N phase-locked loop synthesizer, set from front-panel controls, delivers the RF LO to the STQ2016. A PIC microcontroller handles all the control functions, reading the user controls for setting frequency and mode, displaying these on a front-panel LCD. Weaver/direct-conversion or plain carrier are selectable with USB or LSB direction, the PIC controller driving the lines that go to the dsPic converter module. When switching between Weaver and direct-conversion modes, the frequency from the synthesizer is automatically adjusted by 1800Hz in the appropriate direction for LSB or USB, so the total frequency conversion of the wanted signal remains the same for each mode. The front-panel display then always shows the frequency of the suppressed carrier in the standard way that is common to all SSB transmitters.

The following plots show the 2.4GHz up-converted output when the converter is driven with either broadband noise or a single tone. All the plots have been averaged to smooth-out the displayed noise; the centre frequency of 2400.09MHz and the 30kHz span remain the same in all cases

Figure 3(a) shows the converter output when driven with broadband noise in direct up-conversion mode. The level was set so the red LED was just short of coming on. The response of the input filter can be seen in the band-pass filtered noise, where it forms the two 'brick wall' parts of the upper and lower side-bands in the spectrum display. Side-band rejection can be seen in the difference between heights of the two sections, and can be seen to be a little under 30dB. The nulled carrier leakage is just about discernible, as a small spike on the edge of the noise band, in the centre between the two pedestals.

Figure 3(b) shows the same thing but is now using LSB mode, so the spectrum is reversed. Weaver mode conversion is not shown, since for this noise drive signal it consisted of just a single 'brick wall' with no discernible features, the -30dBc image lying on top of the wanted frequency band, and so completely invisible on the plot.

Figure 4(a) and Figure 4(b) show USB and LSB plots for a single carrier drive at 1kHz, again with the input amplitude set close to maximum. The small noise pedestal around the wanted signal comes primarily from the audio tone generator, a DDS device with a 70dB-specified spurious level, and is filtered by the input band-pass filter. There may also be a contribution from quantisation noise in the dsPic's A/D converter. Although incidental to the plots, this noise pedestal does usefully serve as an indicator of the wanted output pass-band. All frequencies either side of its edges can be regarded as out-of-band with the potential to cause interference. Carrier leakage is more obvious in this plot, and is the small spike at the centre, on the edge of the noise pedestal at around 45dB below the main output 1kHz away. The unwanted side-band 1kHz below the centre is 27dB below the wanted output, consistent with that from the broadband noise plot. The spike on the left-hand side of the USB plot, 3kHz below the centre at 50dB down on the wanted signal, comes from the third harmonic of the drive waveform, and is generated mainly by non-linearity in the mixer. The nature of the quadrature up-conversion process is such that 3rd, 7th and 11th etc harmonic terms appear on the opposite side-band to that in use, while 5th, 9th etc order harmonics appear on the same side as the conversion. These can just be seen in the plots, riding slightly above the noise level.

Figures 5(a) and Figure 5(b) show, respectively, 1kHz and 2.2kHz tones converted using the Weaver mode. To avoid confusion, only upper side-band plots are shown for these two cases, where the two tones are chosen to lie either side of the Weaver central conversion frequency. Recall that the RF source is shifted in frequency by 1800Hz when Weaver mode is selected to compensate for the frequency conversion around the audio centre, ensuring that the final output frequency is exactly the same for either conversion type. Now, carrier leakage in the mixer appears 1.8kHz above the centre of the plot, roughly in the middle of the noise pedestal. The third-order harmonic terms, again on the opposite side of the conversion can be seen in each figure, falling inside or outside the noise pedestal depending on their spacing from the main tone.

The unit has been used for a number of SSB QSOs through QO-100, being the only linear transverter available here for the 2.4GHz band. The VOX proved particularly valuable for ease of use through the satellite transponder.

References

[1] *RadCom*, April 2017, Design Notes page 27.
[2] *RadCom* February 2020, Design Notes page 62.
[3] ADL5375 quadrature up-converter for 400MHz to 6000MHz: https://www.analog.com/en/products/adl5375.html
[4] dsPic code can be obtained on request from the author at andy.g4jnt@gmail.com

Contest Calendar September 2023

Ian Pawson, G0FCT

RSGB HF Events

Date	Event	Times (UTC)	Mode(s)	Band(s)	Exchange
Date	Event	Times (UTC)	Mode(s)	Band(s)	Exchange
Sat 2-Sun 3 Sep	SSB Field Day	1300-1300	SSB	3.5-28	RS + SN
Mon 4 Sep	Autumn Series SSB	1900-2030	SSB	3.5	RST + SN
Wed 13 Sep	Autumn Series CW	1900-2030	CW	3.5	RST + SN
Mon 18 Sep	RSGB FT4 Contest	1900-2030	FT4	3.5, 7, 14	Report
Thu 28 Sep	Autumn Series DATA	1900-2030	RTTY, PSK63	3.5	RST + SN

RSGB VHF Events

Date	Event	Times (UTC)	Mode(s)	Band(s)	Exchange
Sat 2-Sun 3 Sep	144MHz Trophy Contest	1400-1400	All	144	RS(T) + SN + Locator
Sun 3 Sep	5th 144MHz Backpackers	1100-1500	All	144	RS(T) + SN + Locator
Tue 5 Sep	144MHz UKAC	1900-2130	All	144	RS(T) + SN + Locator
Tue 5 Sep	144MHz FMAC	1800-1855	FM	144	RS + SN + Locator
Wed 6 Sep	144MHz FT8 AC (4 hour)	1700-2100	FT8	144	Report + 4-character Locator
Wed 6 Sep	144MHz FT8 AC (2 hour)	1900-2100	FT8	144	Report + 4-character Locator
Tue 12 Sep	432MHz UKAC	1900-2130	All	432	RS(T) + SN + Locator
Tue 12 Sep	432MHz FMAC	1800-1855	FM	432	RS + SN + Locator
Wed 13 Sep	432MHz FT8 AC (4 hour)	1700-2100	FT8	432	Report + 4-character Locator
Wed 13 Sep	432MHz FT8 AC (2 hour)	1900-2100	FT8	432	Report + 4-character Locator
Thu 14 Sep	50MHz UKAC	1900-2130	All	50	RS(T) + SN + Locator
Sun 17 Sep	70MHz AFS Contest	0900-1200	All	70	RS(T) + SN + Locator
Tue 19 Sep	1.3GHz UKAC	1900-2130	All	1.3G	RS(T) + SN + Locator
Thu 21 Sep	70MHz UKAC	1900-2130	All	70	RS(T) + SN + Locator
Tue 26 Sep	SHF UKAC	1830-2130	All	2.3-10G	RS(T) + SN + Locator

Best of the Rest Events

Date	Event	Times (UTC)	Mode(s)	Band(s)	Exchange (Info)
Sat 2 Sep	CWops CW Open	0000-2359	CW	1.8-28	SN + name (three 4-hour sessions)
Sat 2-Sun 3 Sep	All Asian DX	0000-2359	SSB	1.8-28	RS + age (YL send 00)
Sat 2-Sun 3 Sep	IARU Region 1 Field Day	1300-1300	SSB	3.5-28	RS + SN
Sun 3 Sep	WAB 2m QRO Phone	1000-1400	AM, FM, SSB	144	RS + SN + WAB square
Wed 6 Sep	UKEICC 80m	2000-2100	SSB	3.5	6-character Locator
Sat 9-Sun 10 Sep	WAE DX SSB	0000-2359	SSB	3.5-28	RS + SN (Eu works non-EU only)
Sun 10 Sep	UKuG 24-76G	0900-1700	All	24-76G	RS(T) + SN + Locator
Sun 17 Sep	IRTS 70cm Counties	1300-1330	SSB/FM	432	RS + SN + Locator (EI & GI also give county)
Sun 17 Sep	IRTS 2m Counties	1300-1500	SSB/FM	144	RS + SN + Locator (EI & GI also give county)
Sun 17 Sep	BARTG Sprint PSK63	1700-2100	PSK63	3.5-28	SN
Sat 23-Sun 24 Sep	CQ WW DX RTTY	0000-2359	RTTY	3.5-28	RST + CQ Zone (UK = 14)
Sun 24 Sep	UKuG 5.7/10G	0600-1800	All	5.7 & 10G	RS(T) + SN + Locator
Sun 24 Sep	PW 70MHz	1200-1600	All	70	RS(T) + SN + Locator
Wed 27 Sep	UKEICC 80m	2000-2100	CW	3.5	6-character Locator
Sat 30 Sep-Sun 1 Oct	UKEICC DX SSB	1200-1200	SSB	3.5-28	RS + SN (UK/EI also send District Code)

For all the latest RSGB contest information and results, visit www.rsgbcc.org